

Draft Final Report

Protocol for Predicting Long-term Service of Corrugated High Density Polyethylene Pipes

Prepared for the

Florida Department of Transportation

by

Y. Grace Hsuan, Ph.D.,
Drexel University
Civil, Architectural and Environmental Engineering
Philadelphia, PA 19104

Timothy McGrath, Ph.D., P.E.
Simpson Gumpertz & Heger Inc.
41 Seyon St., Building 1, Suite 500
Waltham, Massachusetts 02453

July 29, 2005

Table of Contents

ABSTRACT

CONTENTS

Page

Part I	Evaluation and Control of Stresses in Buried Corrugated HDPE Drain Pipes	1
1.	INTRODUCTION	2
2.	ESTIMATES OF FIELD STRESS LEVELS	2
2.1	CONSIDERATIONS IN DETERMINING STRESS LEVELS	2
2.2	FINITE ELEMENT MODELING	3
2.2.1	FE MODEL	4
2.2.2	PIPE MODEL	7
2.3	SIMPLIFIED DESIGN PROCEDURES	8
2.3.1	AASHTO DESIGN PROCEDURES (AASHTO LRFD SECTION 12.12.3.4)	8
2.4	RESULTS	10
2.4.1	EFFECT OF BACKFILL MATERIAL AND HAUNCH SUPPORT	10
2.4.2	HOOP COMPRESSION STRAIN	12
2.4.3	BENDING STRAIN	14
2.4.4	COMBINED STRAIN	15
2.4.5	DISCUSSION OF RESULTS	16
2.5	LONGITUDINAL STRESSES	17
3.	CONSTRUCTION CONSIDERATIONS	18
3.1	BACKFILL SELECTION	19
3.2	BACKFILL PLACEMENT	21
3.3	BACKFILL COMPACTION	23
3.4	MINIMUM COVER DEPTH	23
3.4.1	PHARES ET AL. (1998)	23
3.4.2	AROCKIASAMY ET AL. (2002)	24
3.4.3	MCGRATH ET AL. (2002)	25
3.4.4	DISCUSSION	26
4.	CONCLUSIONS	27
5.	REFERENCES	28
Part II	Stress Crack Resistance, Oxidation Resistance and Viscoelastic Properties of Corrugated HDPE Pipes	31
1.	INTRODUCTION	32
2.	TEST MATERIALS	32
3.	LABORATORY TESTS TO EVALUATE LONG TERM STRESS CRACK RESISTANCE OF CORRUGATED HDPE PIPES	33
3.1	BACKGROUND	33
3.2	STRESS CRACK RESISTANCE OF CORRUGATED HDPE PIPES	34

3.2.1	STRESS CRACK RESISTANCE OF THE CORRUGATED PIPE LINER	35
3.2.2	STRESS CRACK RESISTANCE OF THE LINER/CORRUGATION JUNCTION	37
3.2.3	STRESS CRACK RESISTANCE OF LONGITUDINAL PROFILES	40
3.3	LONG-TERM STRESS CRACK RESISTANCE OF PIPES	42
3.3.1	TEST ENVIRONMENTS	43
3.3.2	PERFORMANCE TEST FOR ASSESSING SCR OF CORRUGATED HDPE PIPES	47
3.3.3	PREDICTION METHODS	48
3.3.4	COMPARING PSM AND RPM IN PREDICTING	50
3.4	SUMMARY OF LABORATORY SCR EVALUATION	52
4.	LABORATORY TESTS TO EVALUATE OXIDATION RESISTANCE OF CORRUGATED HDPE PIPES	53
4.1	BACKGROUND	53
4.2	METHODS TO EVALUATE ANTIOXIDANTS	57
4.3	ACCELERATED OXIDATION TESTS	59
4.3.1	ACCELERATED OXIDATION IN AIR	59
4.3.2	ACCELERATED OXIDATION IN WATER	60
4.4	DETERMINING THE INITIAL OXIDATIVE INDUCTION TIME VALUE	65
4.5	ASSESSING OXIDATION RESISTANCE	66
4.6	SUMMARY OF LABORATORY OXIDATION RESISTANCE EVALUATION	67
5.	LABORATORY TESTS TO EVALUATE LONG TERM DESIGN PARAMETERS OF HDPE CORRUGATED PIPES	68
5.1	BACKGROUND	68
5.2	TENSILE PROPERTIES OF PIPES	68
5.3	LONG-TERM TENSILE STRENGTH	69
5.4	FLEXURAL MODULUS OF PIPES	71
5.5	LONG-TERM FLEXURAL MODULUS	72
5.6	SUMMARY OF LONG-TERM MECHANICAL PROPERTIES	76
6.	SPECIFICATION	77
7.	CONCLUSIONS	80
8.	REFERENCES	81

List of Tables

	Page
Table 1.1 42-in. Diameter PE Pipe Properties	7
Fig. 1.12 Combined strain at 5% deflection	15
Table 1.2 Energy Required to Achieve Soil Stiffness (McGrath, et al., 1990)	20
Table 1.3 Recommended Minimum Depth of Cover (in.)	27
Table 2.1 Properties of P-1, P-2 and P-3 Pipes	33
Table 2.2 Cell Class Properties for Corrugated HDPE Pipes	34
Table 2.3 Results of NCLS Test of Pipes P-1, P-2, and P-3	36
Table 2.4 Slope Values of Ductile and Brittle Regions from Fig. 2.2	37
Table 2.5 Results of Junction Tests on Pipes P-1 and P-2	39
Table 2.6 Results of Longitudinal Profile Tests at Vent Holes	41
Table 2.7 Information Obtained from Ductile-to-Brittle Curves in Water	44
Table 2.8 Information Obtained from Ductile-to-Brittle Curves in Air	45
Table 2.9 Properties Obtained from the Ductile-to-Brittle Curves in Fig. 2.12	48
Table 2.10 Mechanical Properties for Design Corrugated HDPE Pipes	68
Table 2.11 Type of Die used in ASTM D 638 for Different Pipe Diameters	69
Table 2.12 Average Tensile Yield Strength from Molded Plaque and Pipe Liner	69
Table 2.13 Flexural Modulus obtained from DMA tests	76
Table 2.14 Interim Specification for Long-Term Performance of Corrugated HDPE Pipes	78
Table 2.15 Full Specification for Long-Term Performance of Corrugated HDPE Pipes	79

List of Figures

	Page	
Fig. 1.1	Finite element mesh	5
Fig. 1.2	Soil zones	5
Fig. 1.3	Construction increments	6
Fig. 1.4	Deflection versus depth of fill, soil type and compaction	11
Fig. 1.5	Thrust in pipe wall versus depth of fill, soil type and compaction	11
Fig. 1.6	Comparison of haunched and unhaunched bending strains	12
Fig. 1.7	Axial strain at 3% deflection	13
Fig. 1.8	Axial strain at 5% deflection	13
Fig. 1.9	Bending strain at 3% deflection	14
Fig. 1.10	Bending strain at 5% deflection	14
Fig. 1.11	Maximum combined strain at 3% deflection	15
Fig. 2.1	Schematic diagram illustrating the location of circumferential cracking in corrugated HDPE pipes	35
Fig. 2.2	Location of the test specimens taken from the pipe liner	36
Fig. 2.3	Ductile-Brittle curves of three tested pipes, P-1, P-2 and P-3	37
Fig. 2.4	Locations of SCR junction specimens taken from junction width less than 1.0 inch	38
Fig. 2.5	Locations of SCR junction specimens taken from junction width greater than 1.0 inch	38
Fig. 2.6	Failure of junction-specimen from pipe P-1	39
Fig. 2.7	Failure of junction-specimen from pipe P-2	40
Fig. 2.8	Specimen configuration for vent hole location	41
Fig. 2.9	Failed longitudinal profile (vent hole) specimen	42
Fig. 2.10	Applied stress versus failure time curves of P-3 in water	44
Fig. 2.11	Applied stress versus failure time curves of P-3 in air	45
Fig. 2.12	Ductile-to-brittle curves in three different test environments at 50°C	46

Fig. 2.13	Applied stress versus failure time curves for junction tests of P-1	47
Fig. 2.14	Experimental and predicted NCLS curves on pipe liner in water	50
Fig. 2.15	Experimental and predicted NCLS curves on pipe liner in air	51
Fig. 2.16	Experimental and predicted curves on pipe junction in water	51
Fig. 2.17	Predicted 23°C curve on pipe junction in water	52
Fig. 2.18	OIT data of fourteen commercially new pipe samples	53
Fig. 2.19	Three conceptual oxidation stages of HDPE	55
Fig. 2.20	Three potential failure stages in pressure testing of smooth wall pipes	55
Fig. 2.21	Depletion of antioxidants with time for five HDPE geomembranes with unknown antioxidant formulations	56
Fig. 2.22	Correlation between OIT and IT of four polyethylene grades	58
Fig. 2.23	Correlation between IT and OIT	58
Fig. 2.24	OIT depletion curve of P-1 in a forced air oven at 85°C	60
Fig. 2.25	OIT depletion curve of P-2 in a forced air oven at 85°C	60
Fig. 2.26	OIT depletion curves in air and water at 85°C of P-1	61
Fig. 2.27	OIT depletion curves in air and water at 85°C of P-2	62
Fig. 2.28	Material properties of P-1 versus incubation time in water at 85°C	62
Fig. 2.29	Material properties of P-2 versus incubation time in water at 85°C	63
Fig. 2.30	Three conceptual degradation stages in air and water incubation	63
Fig. 2.31	FTIR spectra of sample P-1 after incubation in 85°C water for 2341 hours	64
Fig. 2.32	Plot $\ln(\text{OIT})$ versus predicted lifetime	66
Fig. 2.33	Hydrostatic burst pressure test data on smooth HDPE pipes	70
Fig. 2.34	Obtaining master curve by shifted data in Fig. 2.34 to 20°C	71
Fig. 2.35	Configuration of specimen clamping system in DMA	73
Fig. 2.36	Deformation of the test specimen in DMA	73
Fig. 2.37	Stress relaxation curves resulted from the DMA test-1	74
Fig. 2.38	Master curve at 27.5°C after shifting using the T-T-S software	75

Fig. 2.39	Master curve at 27.5°C after shifting using Popelar factors	75
Fig. 2.40	Master Curve at 27.5°C from DMA test-2	76

ABSTRACT

The Florida Department of Transportation (FDOT) retained Simpson Gumpertz & Heger Inc and Drexel University to develop testing and analysis protocols that can assess pipe properties and design procedures to ensure 100-year service life of HDPE corrugated pipes. The report consists of two parts; Part I presents the results of Simpson Gumpertz & Heger Inc. (SGH) study on pipe stress and construction protocol while Part II presents the results of Drexel University study on long term properties of the respective pipes.

Part I of the project utilized a finite element model to analyze buried corrugated HDPE pipe under earth loads with several compaction conditions, depths of fill, and variable support under the pipe haunches. It indicated that long-term service tensile strain in the pipe should be less than 1.6%, corresponding to a long-term stress of approximately 320 psi. This is significantly reduced from the current AASHTO requirement of 5% long-term service tensile strain capacity. Studies on three-dimensional analysis of longitudinal strains in corrugated profiles indicate that the same minimum tensile stress capacity should also apply to longitudinal stresses. Applying a factor of safety of 1.5 to the service level stress requires that the minimum 100 year tensile strength of the pipe should be equal, or less than, 2.5% strain, or about 500 psi.

To provide good performance the required controls on construction procedures backfill materials should be limited to well-graded, coarse-grained soils (sands and gravels) with less than 12% fines. Uniform coarse-grained soils provide good performance but need to be checked for the likelihood of migration of fines into open voids. Uniform fine sands should be avoided. Coarse-grained soils with fines or fine grained soils with at least 30% coarse grained material provide good performance if placed and compacted properly, but increased inspection during construction is recommended. Backfill should be compacted to at least 95% of maximum standard Proctor density for applications in roadways.

The most important aspect of construction control requires inspection of buried corrugated PE after installation. Total reduction in vertical diameter should be measured and limited to 5%. On large projects, deflections should be evaluated after a small portion of the project has been completed to determine if the construction procedures are adequate.

Minimum cover for applications subjected to live loads should be 2 ft or one-half diameter, whichever is greater.

Part II of the project focused on four material properties. They were stress crack resistance (SCR), oxidation resistance (OR), long-term tensile strength, and flexural modulus. The evaluation targeted the finished pipe properties so that effects of the manufacturing processes and pipe profile designs were included.

For SCR properties, the effects of manufacturing processing were observed in pipe liner tests. Also, pipe junctions and vent holes were found to be susceptible to stress cracking, but the sensitivity varied with the pipe design. The long-term performance test to assess SCR of the pipe was evaluated using junction specimens in a water environment. Elevated temperatures were utilized to accelerate the crack growth rate so that the SCR properties at a site temperature of 23°C could be predicted. Two predicting methods, the Popelar Shift Method (PSM) and the Rate Processing Method (RPM), were examined for their applicability. Results from both notched liner and junction tests indicated that RPM is a more reliable method to predict the SCR behavior from elevated temperatures to low site temperature. Two test methods (FM 5-572 and FM 5-573) were developed for the SCR tests and to predict long-term crack resistance.

The oxidation resistance of the corrugated HDPE pipes was evaluated based on both antioxidant depletion and degradation of polyethylene. The antioxidant content and depletion rate in the pipes were assessed using oxidative induction time (OIT) test after water incubation. A minimum OIT value for new unaged corrugated HDPE pipes was established to be 25 minutes. In addition, the maximum antioxidant depletion rate was determined by water immersion at 85°C for a duration of 187 days. The OIT retained value of the 187-day incubated specimen shall be at least 3 minutes. The step-by-step test procedure to predict lifetime of antioxidants and corrugated pipes was developed in the test method designated FM5-574.

The long-term design parameters (tensile strength and flexural modulus) are predicted using the Time-Temperature Superposition (TTS) method. A tensile creep rupture test was utilized to determine the 100-year tensile strength of the corrugated pipe, while a stress relaxation test on the finished pipe was used for the 100-year flexural modulus. Three new test methods, FM5-

Draft Final Report

575, FM5-576 and FM5-577, were developed to describe the test procedures for the determining 100-year tensile strength and modulus values.

As a result of the study, an interim specification was developed to be implemented for HDPE corrugated pipes. It includes requirements for stress cracking resistance and oxidation resistance. Also a full specification was recommended in which the long-term tensile strength and modulus are included.

Draft Final Report

Preamble

PART I - Evaluation and Control of Stresses in Buried Corrugated HDPE
Drain Pipes

1. INTRODUCTION

As the cost of highway construction increases, transportation engineers are increasingly looking to extend the design life of highways and bridges to provide longer service without reconstruction. The AASHTO LRFD Bridge Design Specifications (AASHTO LRFD, 1998) state that the design life of bridges should be 75 years. This code also governs the design of culverts. The Florida Department of Transportation (FDOT) requires design of structures for a 100 year service life, raising questions about the performance of thermoplastic pipes, which currently have 50 year properties listed in AASHTO LRFD. The questions pertain to the determination of long-term performance of thermoplastics, which have time dependent properties, and to the strain demand on the pipes, which is also time dependent. Of particular interest to FDOT is corrugated HDPE pipe. This report addresses the stress and strain demand on corrugated HDPE and on construction materials and procedures that can be used to reduce the demand.

2. ESTIMATES OF FIELD STRESS LEVELS

2.1 Considerations in Determining Stress Levels

Determining the stress level in buried pipes can be accomplished through several techniques, with varying degrees of sophistication. It has been our experience that the field control exercised during installation of buried pipes is minimal and the variability is high. Simplified design procedures are normally applied with conservative assumptions, producing designs that are adequate for typical applications. More sophisticated procedures, such as finite element analysis (FEA) are normally used only for research, large culvert sizes, or special applications where the cost of the more detailed analysis is justified through economy of fabrication or installation that can be achieved using less conservative (hence more accurate) design assumptions, and where the cost of field inspection to insure that the design assumptions are met, can be justified.

This section examines, and modifies as necessary, the simplified design procedures used by AASHTO for calculation of stress levels in buried pipe, and compares those results with predictions of FEA models. The results of these two methods are used to determine stress levels that are likely to occur in buried pipe when in service for 100 years.

This analysis is undertaken to determine the maximum tensile stress that may occur in a pipe in service for a period of 100 years. The total stress in a pipe is a combination of the bending stress that results from changes in the shape of the pipe (most commonly represented by vertical deflection), and the hoop compression stress that results from external soil loads. Total stress is most often represented as:

$$\sigma = P / A \pm M c / I \quad \text{Eq. 1.1}$$

where:

- σ = stress in pipe wall, psi
- P = hoop thrust in pipe wall, lb/in.
- A = cross-sectional area of pipe wall, in.²/in.
- M = moment in pipe wall, in.-lb/in.
- c = distance from centroidal axis to extreme fiber of pipe wall, in
- I = moment of inertia of pipe wall, in⁴/in.

In buried pipe, the hoop thrust stress is always compression. Bending produces tension stresses on one surface and compression stresses on the other. To estimate the maximum tension stress in the pipe wall, the hoop thrust stress (P/A) is combined with the maximum tension stress produced by bending (Mc/I). It is important to recognize that:

- since tension is produced only by pipe deflection, it is important to control pipe deflection during installation,
- if the hoop thrust stress is large relative to bending, there may be no tension in the pipe, and
- the highest tension stress will occur in a shallow buried pipe (low thrust) with high deflection (high bending).

2.2 Finite Element Modeling

Finite element modeling was undertaken using the computer program CANDE. This program was developed by the US Federal Highway Administration specifically for analysis of buried pipes. The program is publicly available. The specific version of CANDE used was CANDECad. This version uses the CANDE program for calculations, but adds an Autocad based pre- and post-processor, which facilitates the modeling process.

2.2.1 FE Model

The finite element mesh used in the analysis is presented in Fig. 1.1. Figs. 1.2 and 1.3 show the soil zones and the construction increments used in the analysis, respectively. All analysis was completed using an embankment installation, since this generally produces more load and deflection than a trench installation.

Soil properties were those developed by Selig (1988). These properties use the hyperbolic Young's modulus developed by Duncan et al. (1980) and the hyperbolic bulk modulus developed by Selig (1988). There are three general groups of placed backfill soils in this set of properties, which are defined in AASHTO LRFD (1998) Table 12.12.2.4-2. These groups are coarse-grained soils with little or no fines (Sn), coarse-grained soils with fines or sandy or gravelly fine-grained soils (Si) and fine-grained soils (Cl). General assumptions for soils used in the analyses were:

- native soil under the pipe was considered to be a firm fine-grained material,
- a small area (Zone 5, called the "void") which is difficult to compact in the field was always considered to be filled with a very soft material (silty material at 50% of standard Proctor density, called Si50),
- a larger area under the pipe (Zone 6, called the "haunch zone") is considered filled with backfill soil if the pipe model is assumed to be haunched, and is filled with Si50 material if the model is assumed to have poor haunching,
- four conditions of structural backfill (Zone 3) were used; most analyses were completed with a coarse-grained material compacted to 90% of standard Proctor density (Sn90), a silty material compacted to 90% of standard Proctor density (Si90), and a silty material compacted to 85% of standard Proctor density (Si85); some analyses were also conducted with Si80 backfill; Zones 2 and 7 were modeled as structural backfill since the installations were modeled as embankment conditions, and
- the pipe bedding (Zone 4) was modeled as Si90 for all installations.

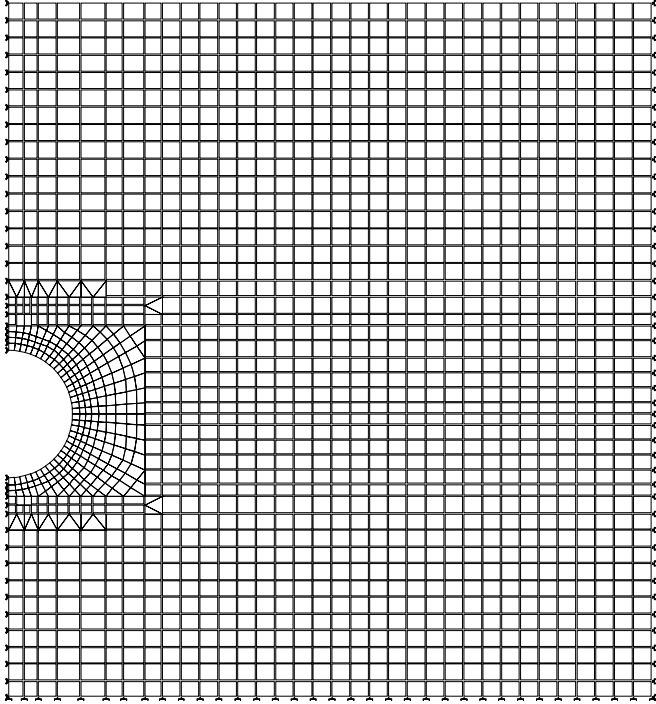


Fig. 1.1 – Finite element mesh

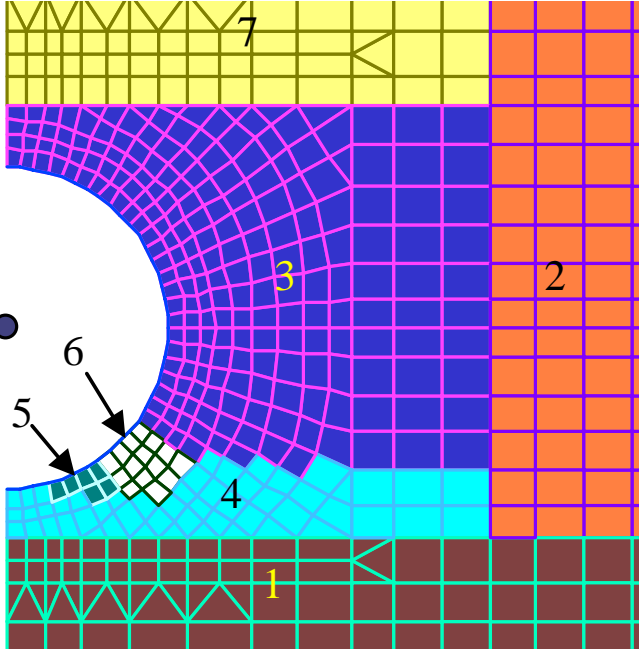


Fig. 1.2 – Soil zones

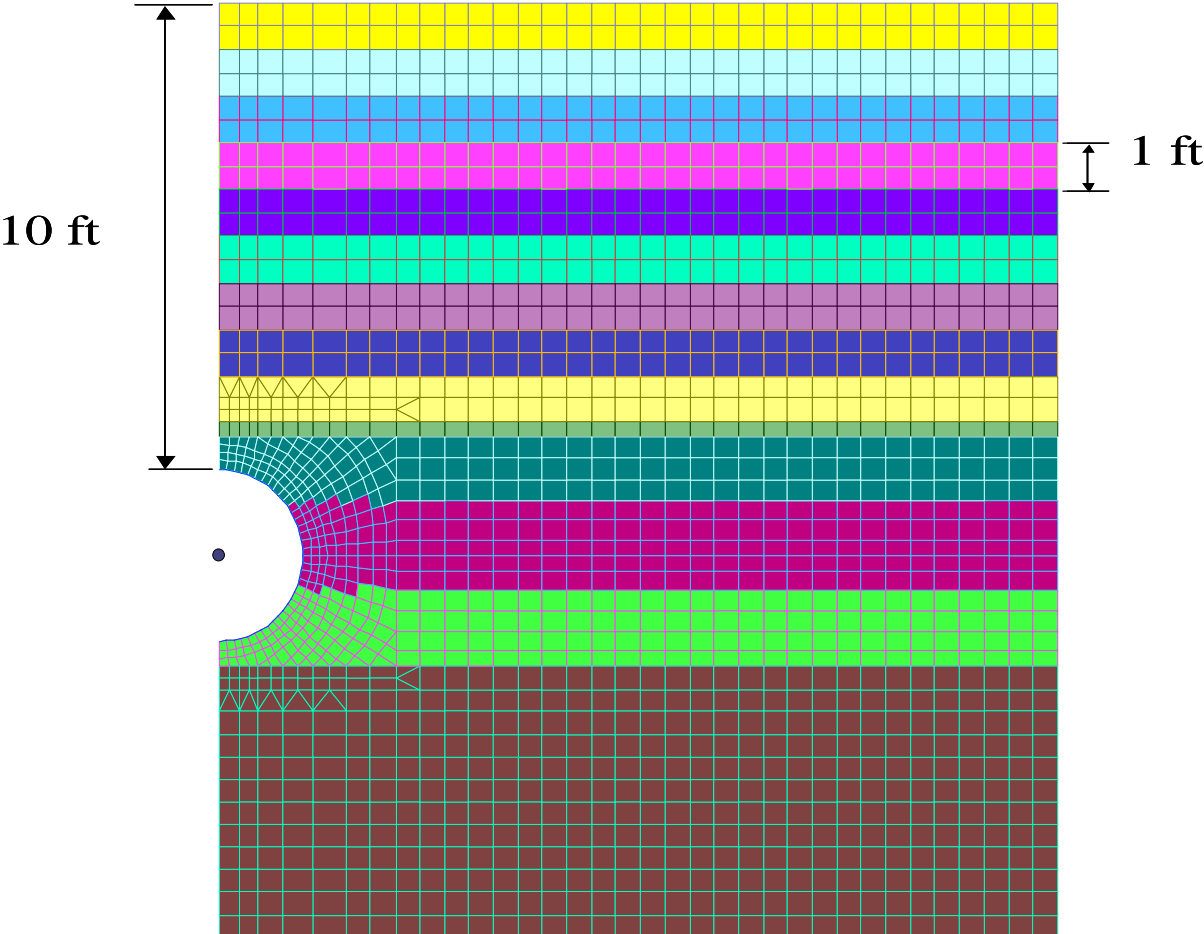


Fig. 1.3 – Construction increments

The model assumes that the pipe-soil interface was a no-slip (bonded) condition. This results in higher estimates of thrust at the springline and lower estimates of thrust at the crown than the full-slip (frictionless) condition. The AASHTO procedures for thrust design (AASHTO LRFD) are based on a mix of the no-slip and full-slip conditions (McGrath, 1999). For this study, the focus is on an estimate of the minimum hoop compression stress, thus, as noted in Section 2.3, the simplified thrust computed by AASHTO procedures should be reduced.

The coarse-grained material represents a high quality backfill with a relatively high soil modulus that can be achieved with little compactive effort. Densities of coarse-grained materials are often as high as 85% of maximum standard Proctor when dumped without compaction. The silty materials represent soils that can achieve good stiffness if compacted, but require more site control of moisture content and compactive effort. Silty soils have low stiffness if left in a dumped condition. No clay soils were considered, since these materials have marginal stiffness when compacted and require considerable controls during installation.

Analyses were completed for depths of fill from 2 ft to 21 ft.

2.2.2 Pipe Model

Most FE modeling was completed assuming a 42 in. diameter pipe. The section properties used in the analysis are presented in Table 1.1.

Table 1.1 – 42-in. Diameter PE Pipe Properties

Property	Value
Inside Diameter	42 in.
Profile Height	2.93 in.
Depth from outside surface to centroid	1.91 in.
Area	0.41 in. ² /in.
Moment of Inertia	0.45 in. ² /ft

The profile considered has the centroid eccentric from the mid-height of the profile. This produces relatively high bending strains when the pipe deflects. This condition is typical of many corrugated PE profiles available today; however, some profiles are now available with the

centroid located near the mid-height of the profile and producing lower bending strains for the same deflection. The analysis results are generally applicable to all corrugated HDPE pipes.

All analyses were completed using an estimated long-term modulus of 20,000 psi, which results in good predictions of long-term thrust forces. This approach results in lower pipe stiffness during placement of backfill, but previous research, and elastic theory have demonstrated that the affect on deflection and bending is not significant.

2.3 Simplified Design Procedures

2.3.1 AASHTO Design Procedures (AASHTO LRFD Section 12.12.3.4)

Simplified analysis procedures presented here are based on the AASHTO design method for thermoplastic pipe (AASHTO, 1998) with some modifications. The AASHTO design procedure was developed to predict the maximum hoop compression in the pipe wall for the purpose of obtaining a conservative design for general and local buckling. Modifications are required to the thrust effects to predict maximum likely tension stress.

2.3.1.1 Hoop Thrust Compression Strain

Hoop thrust compression strain is computed as:

$$\varepsilon_T = 0.5 W_{sp} VAF/EA \quad \text{Eq. 1.2}$$

where:

ε_T = hoop compression strain

W_{sp} = soil prism load, lb/in

$$= \gamma_s D_o (H + 0.11 D_o)$$

VAF = vertical arching factor to account for pipe-soil interaction

$$= 0.76 - 0.71 (S_H - 1.17) / (S_H + 2.92)$$

S_H = hoop stiffness factor

$$= \phi_s M_s R / E A$$

D_o = pipe outside diameter, in.

H = depth of fill over pipe, in.

γ_s = soil unit weight, lb/in.³

ϕ_s = resistance factor to account for reduced soil stiffness, taken as 0.9

M_s = constrained soil modulus, psi, (See AASHTO LRFD, Table 12.12.2.4-1)

- R = radius to centroid of pipe wall, in.
- E = modulus of elasticity of pipe material, psi, taken as 20,000 psi for long-term
- A = area of pipe wall, in.²/in.

Two modifications were used to estimate the minimum compression stress around the pipe wall:

- to account for variation around the circumference, all thrusts were multiplied by a factor of 0.4 (see Section 2.4 Results for the basis of this)
- to account for local buckling, reduction of wall area was calculated once and not updated. The effective area varied from 0.95% of the total area at a depth of 2 ft, to 80% of the total area at a depth of 20 ft (AASHTO LRFD 12.12.3.5.3).

For shallow installations, there is some debate whether soil arching, as predicted for deep installations, will occur for shallow installations. Since the need is to predict the minimal possible thrust, arching is considered as it reduces the load on the pipe.

2.3.1.2 Bending Strain (AASHTO LRFD 12.12.3.5.4b)

Bending strain was approximated using the AASHTO equation:

$$\epsilon_B = D_f (\Delta_b/D) (c/R) \quad \text{Eq. 1.3}$$

where:

- ϵ_B = bending strain in pipe wall
- D_f = shape factor to account for distortion during installation, taken as 4.0
- Δ_b/D = pipe deflection due to bending, expressed as a ratio to the pipe diameter to the centroid of the pipe wall
- c = distance from centroid of pipe wall to extreme fiber of pipe wall, in., (use c_{in} or c_{out} as appropriate to calculate tension stress)
- R = radius to centroid of pipe wall, in.

Total deflection, expressed as a ratio of the change in vertical diameter to the inside diameter, is the sum of the hoop compression strain and the vertical bending deflection:

$$\Delta_T/D = \Delta_b/D + \epsilon_T \quad \text{Eq. 1.4}$$

Since field control is based on total deflection, the approach taken in computing bending strain was to:

- select a target deflection at a given depth of fill,
- compute expected hoop thrust strain at that depth,
- compute bending deflection by subtracting the hoop thrust strain from the target deflection, and
- compute the bending strain based on the bending deflection.

The calculations presented in the subsequent sections are all based on total deflection, which is the sum of the hoop thrust strain and the bending strain due to deflection.

A sample calculation is presented in Appendix A.

2.4 Results

2.4.1 Effect of Backfill Material and Haunch Support

For the three backfill materials, Figs. 1.4 and 1.5 show the finite element predictions for deflection and hoop thrust versus depth of fill. This demonstrates the significant loss of stiffness as the backfill has more fines (i.e. silty, Si, versus coarse-grained soil, Sn), and/or less compaction. The thrust in the Si85 soil is almost twice that of the pipe in Sn90 soil and the deflection in the pipe in Si85 soil is more than twice that of the pipe in Sn90 soil. The pipe in Si90 soil shows intermediate results.

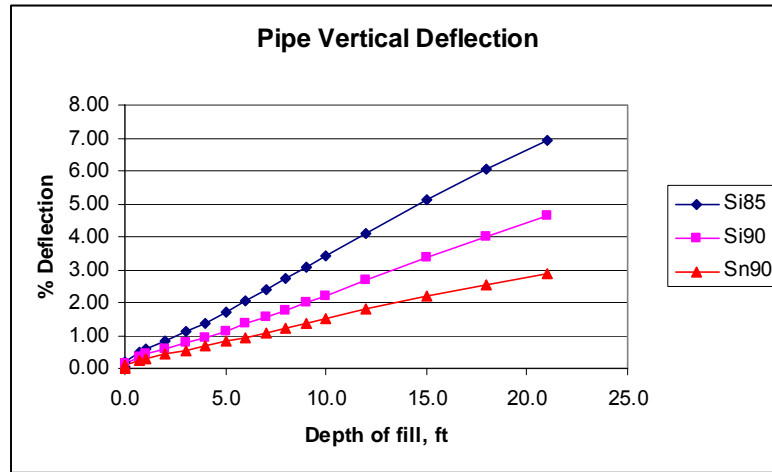


Fig. 1.4 – Deflection versus depth of fill, soil type and compaction

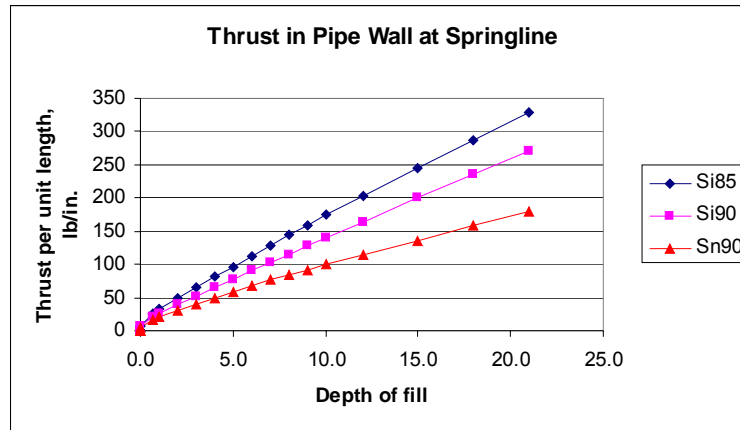


Fig. 1.5 – Thrust in pipe wall versus depth of fill, soil type and compaction

Fig. 1.6 shows the maximum tension bending strains at 3% deflection for pipe in different backfills and with and without haunching support. The figure demonstrates:

- at a given deflection the bending strains are quite similar regardless of the type of backfill if the support conditions are the same.
- haunch support substantially reduces the peak bending strains,
- haunch support only affects bending strain in the invert region, and
- the depths at which 3% deflection occurs varies widely, from 6 ft for a Si80- backfill to 21 ft for a Sn90 backfill.

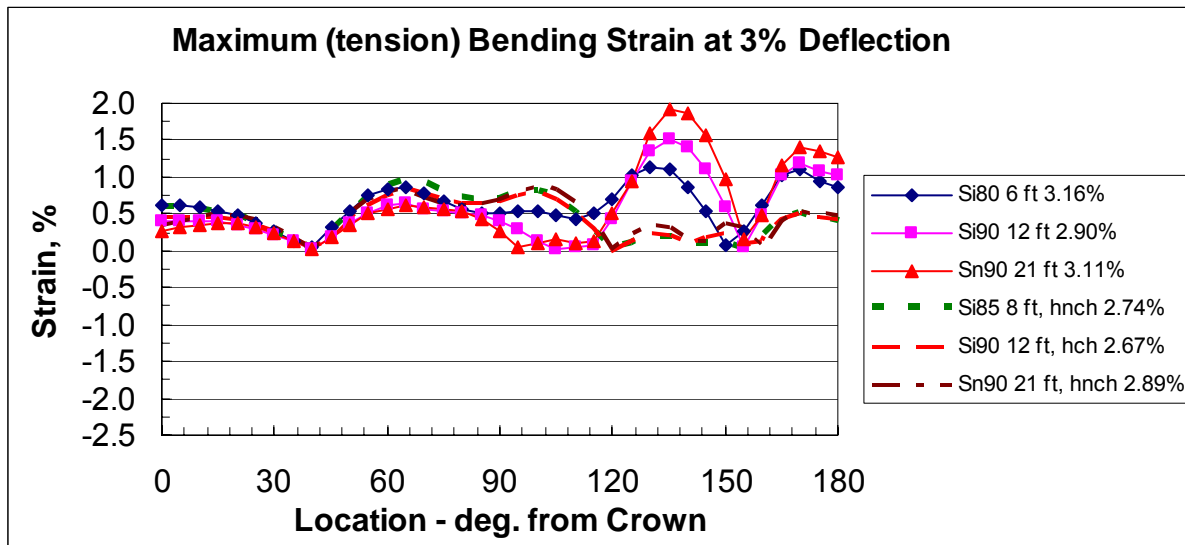


Fig. 1.6 – Comparison of haunched and unhaunched bending strains

2.4.2 Hoop Compression Strain

Fig. 1.7 shows the hoop compression strain for the three backfill conditions at 3% deflection. In this section, and subsequent sections, the deflection considered is the total deflection, that is, the sum of deflection due to bending and hoop compression. Fig. 1.8 makes the same comparison for the Si90 and Si85 backfill at 5% deflection (the Sn90 backfill condition did not reach 5% deflection at a depth of 21 ft. The figures show a variation in the axial strain around the circumference, high at the springline and low at the crown.

The figures also show that the simplified method, with the modifications noted above, gives a reasonable estimate of the minimum hoop stress around the circumference.

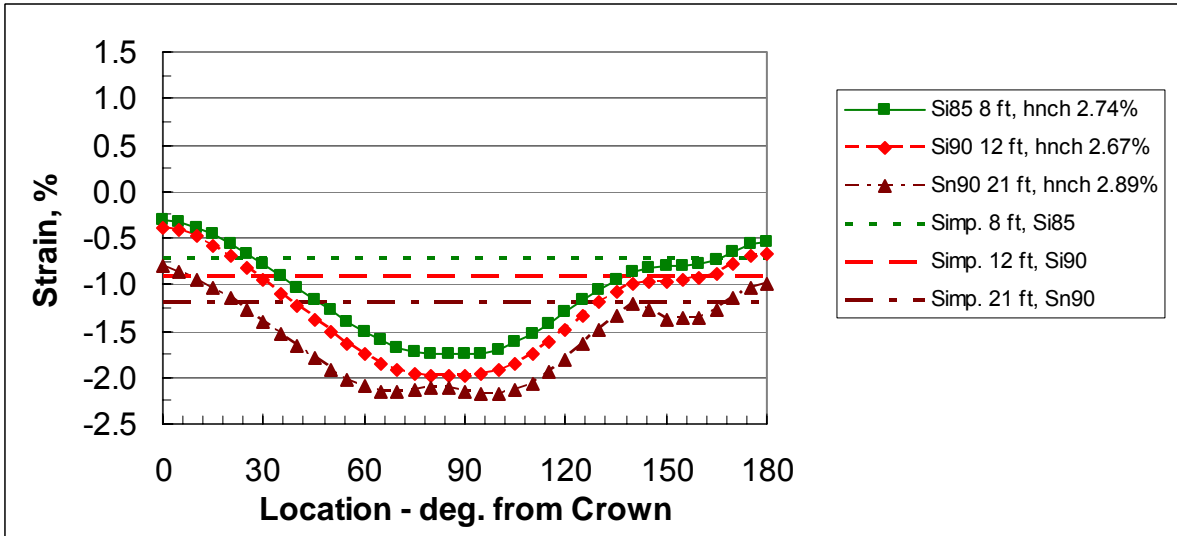


Fig. 1.7 – Axial strain at 3% deflection

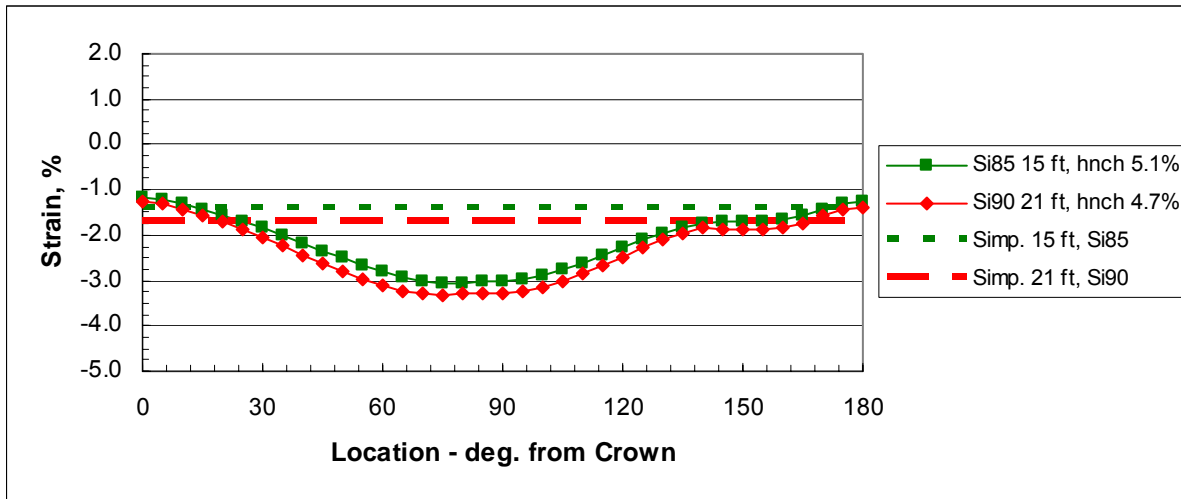


Fig. 1.8 – Axial strain at 5% deflection

2.4.3 Bending Strain

Figs. 1.9 and 1.10 show the bending strain for the haunched pipes at 3% and 5% deflection respectively. The figure shows that the simplified design procedures provide reasonable estimates of the maximum bending strains.

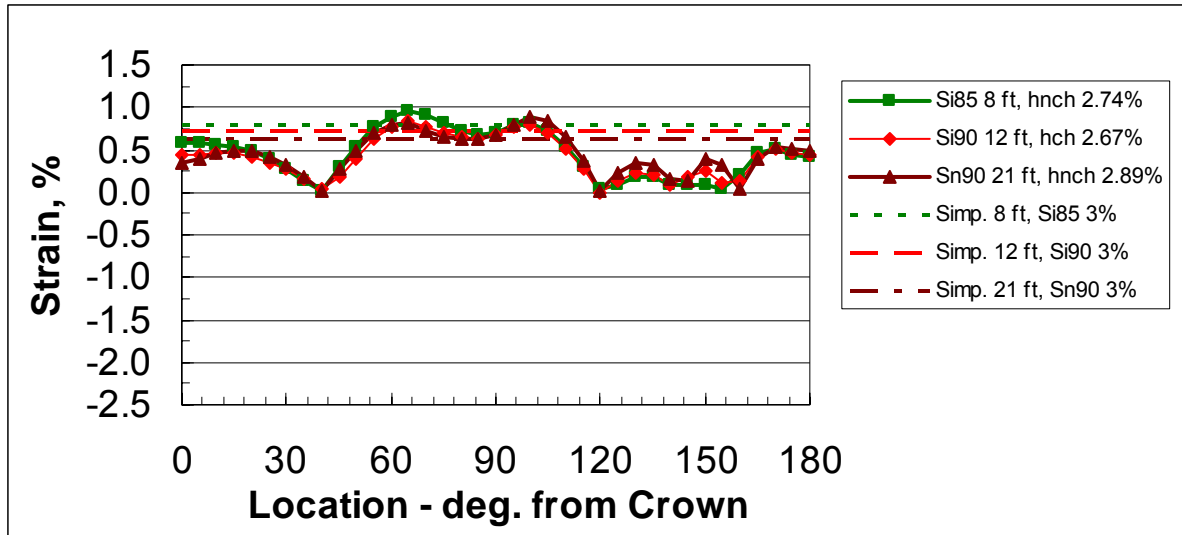


Fig. 1.9 – Bending strain at 3% deflection

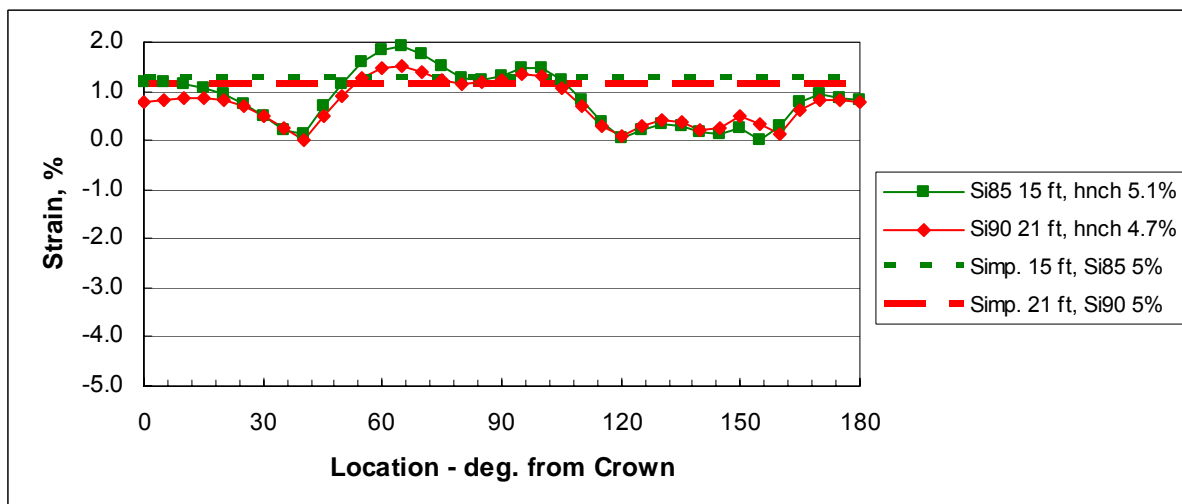


Fig. 1.10 – Bending strain at 5% deflection

2.4.4 Combined Strain

Figs. 1.11 and 1.12 compare the simplified predictions with the FEA results for total combined strain. The comparison suggests that the simplified procedures can be used to predict total pipe strains for the purpose of estimating the demand on the PE material in service.

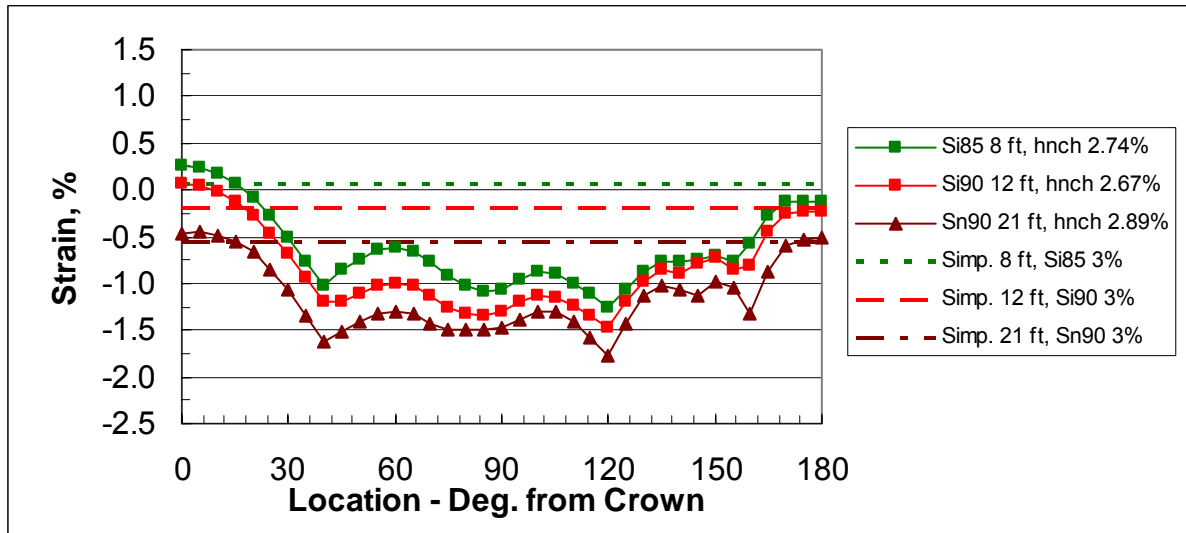


Fig. 1.11 – Maximum combined strain at 3% deflection

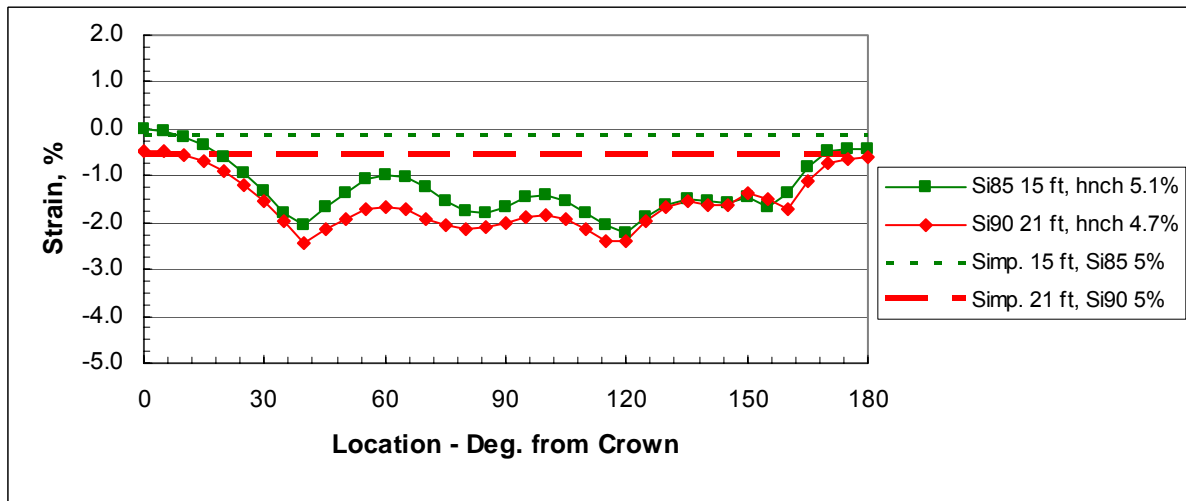


Fig. 1.12 – Combined strain at 5% deflection

2.4.5 Discussion of Results

The pipe performance calculations presented in the previous section show that tensile strains at limiting deflection conditions are low when the deflection is caused by an earth load. Further, as the deflection increases, the tensile strains decrease since the hoop compression strain increases at a faster rate than the bending strain, even for the relatively soft Si85 condition. This indicates that the maximum tension strains in corrugated HDPE pipe will likely occur in shallow buried pipe installed at limiting deflection. There is a bit of a conflict in this finding, since:

- if good construction practices are applied, high deflections should not occur at low depths of fill; however,
- construction control procedures for thermoplastic culverts are generally written to limit deflection to a 5% change in diameter, regardless of the depth of fill

The first bulleted item suggests that tension should not occur in buried HDPE pipe at any depth of fill, but the second item shows that deflections are not controlled to lower limits under shallow burial. Also, research has shown that final deflections in flexible pipe often are greatly affected by construction practices (Chambers et al. 1980 and Chambers and McGrath, 1981) and can significantly exceed values predicted by pipe-soil interaction theory. The author has personally observed a number of installations with high deflections under very shallow conditions.

The result of this is the conclusion that either of two design situations should be selected:

- design for a limiting deflection (i.e. 5%) at a low depth of fill or
- reduce the allowable deflection of pipe under low fill conditions.

Since the latter solution would be difficult to control in a field environment, designing for a 5% deflection with little or no thrust is a preferred solution. Using the simplified procedures for predicting bending strain, this suggests that the limiting strain for the 42 in. pipe used in the FEA study should be:

$$\varepsilon_b = D_f \Delta/D (c_{out}/R) = 4 (0.05) (1.91 \text{ in.} / 22.0 \text{ in.}) = 1.7\%$$

Assuming a 100 year modulus of 20,000 psi this value relates to a stress of 350 psi. The actual value will vary for different profiles as a function of the profile geometry. Overall, since some thrust will always be present in a profile, a strain limit for circumferential effects of 1.5% (equivalent to a long-term stress of 300 psi) appears reasonable at this time. Applying a factor of safety of 1.5 gives strength limits of approximately 500 psi and 2.5% strain.

2.5 Longitudinal Stresses

The simplified calculations and the FEA study address only the circumferential stresses in HDPE pipe. A relationship to stresses in all directions in the profile is required to assess the total stress state and estimate the material performance. Two papers in the literature address longitudinal stress due to earth loads:

- Moore and Hu (1995) studied the three dimensional response of corrugated HDPE under pure compression and reported a peak longitudinal tensile stress of 58 psi at an applied stress of 5 psi, roughly equivalent to 6 ft of fill. The longitudinal tension stress occurs on the inside surface of the pipe where the liner meets the corrugation and inspection of the overall stress distribution suggests that this tension occurs as a local bending of the liner. Using simple extrapolation, the peak longitudinal tension stress at depths of 20 ft would be 193 psi.
- Moore (1995) studied the three-dimensional response of corrugated HDPE pipe in Sn95 and Sn85 (roughly equivalent to Si90 material) structural backfill under deep fills. They reported maximum longitudinal tension of about 200 psi at the springline in Sn85 backfill at depths of about 12 ft. The tension at the crown and invert are much lower. The location of the peak tension, at the intersection of the liner and corrugation, is the same as in the hoop compression test, and local bending again appears to be the cause. This paper presents only combined stresses, thus the separate effects of bending and axial compression in causing longitudinal tension is not clear. Using simple extrapolation, the longitudinal stress at a depth of fill of 20 ft would be about 330 psi.

NCHRP Report 429 (Hsuan and McGrath, 1999) showed that the intersection of the liner and corrugation was the site of a high percentage of cracks in corrugated HDPE pipe; however, they concluded that the cracks initiated on the interior of the corrugation where the profile has a sharp discontinuity, while Moore indicates that the longitudinal stresses at this location are in

compression. Also, as a result of NCHRP Report 429, AASHTO improved the crack resistance of HDPE resins, which was intended to reduce the cracking that was observed.

The other source of longitudinal stress is improper installation, resulting in beam bending type loadings. To control this in the field, Florida will require that pipe grade be controlled to 0.5%. This criterion is applied by assuming that the center of a section of pipe is out of line by 0.005 times the pipe length. Corrugated PE is manufactured in 20 ft lengths, so the criterion allows a deflection of 1.2 in. in a 20 ft span. Assuming that the liner forms a straight tube down the center of a pipe, then, at 0.5% grade misalignment the longitudinal pipe strain is approximately 0.75% or 150 psi in the long-term. As this simplification is conservative, and tension stress due to beam bending will be localized, the two effects need not be considered simultaneously. Thus, HDPE material in corrugated pipe should be able to survive long-term longitudinal tensile stresses of about the same magnitude as circumferential stresses, 300 psi for the service condition, equivalent to approximately 1.5% strain, to provide a 100 year service life.

Note that for both longitudinal and circumferential stresses, the peak stresses do not occur at locations subject to the effects of stress concentrations, thus, the general field capacity of the pipe should be evaluated against this criterion rather than the strength of the pipe at points of stress concentration. The provisions for control of stress cracking are assumed to provide protection at these locations.

3. CONSTRUCTION CONSIDERATIONS

Achieving 100 year service life in HDPE pipe requires control of tensile stresses, which are directly related to deflection. Deflections are controlled by backfill selection and control of construction practices. The finite element analysis demonstrates the role of backfill type and compaction in controlling deflections, but the failure to use good practices during backfill placement can increase deflections significantly above values predicted by pipe-soil interaction analysis. Since deflections are in fact controlled more by construction practice than by design, it is increasingly becoming practice to place responsibility for control of deflections on the contractor, rather than the designer. The design process demonstrates that a pipe is adequate at a given deflection and the contractor is then responsible for meeting that deflection level. Construction practices that produce good pipe performance with minimal inspection and construction control are desirable. Key considerations in this are:

- backfill material
- placement procedures
- compaction procedures, and
- on wet sites, control of ground water to allow proper placement and compaction of backfill.

This section on discussion of suitable backfill materials is generally applicable to all types of pipe.

3.1 Backfill Selection

Backfill placement procedures normally require density control to provide the desired backfill properties. Thus, it is common practice to speak of soil properties and relate them to a given percentage of maximum density determined in accordance with a standardized laboratory reference test. The most common tests are the standard Proctor test (AASHTO T99, ASTM D 698) and the modified Proctor test (AASHTO T180, ASTM D 1557). The modified Proctor test applies approximately four times more energy to the soil and thus achieves a higher reference density. For simplicity, references to percent of maximum density in this report refer to the standard Proctor test. For buried pipe, the property of actual interest is the soil stiffness. The ability of a given soil at a given density to resist deformation of a buried pipe is the key mechanism in controlling deflection.

Coarse-grained backfill materials with limited fines (material passing a #200 sieve) content have the highest initial stiffness without compaction and reach the highest stiffness with the least energy. The relative amount of energy to achieve a level of stiffness in various soils is presented in Table 1.2 (McGrath et al., 1990) based on tests of soils in compaction molds. The table demonstrates that to achieve a soil modulus (in this case expressed as the empirical modulus of soil reaction, E'), of 1,000 psi, requires 3 times more energy applied to a Si soil than a Sn soil, and 7 times more energy in a Ci soil than a Sn soil. In common tables of soil moduli (Howard, 1996), only the Sn soils reach a modulus of 3,000 psi.

Table 1.2 – Energy Required to Achieve Soil Stiffness (McGrath, et al., 1990)

Soil Type	Modulus of Soil Reaction, E', (psi)			
	400	1,000	2,000	3,000
Coarse grained soils, ≤ 12% fines (AASHTO Sn soils, Note 2)	≤5	10	17	30
Sandy or gravelly fine grained soils, or coarse-grained soils with fines (AASHTO Si soils, Note 2)	25	33	40	≥100
Fine grained soils (AASHTO Cl soils, Note 2)	50	70	≥100	≥100

Notes: 1. Energy expressed as a percentage of the energy specified in AASHTO T99

2. See AASHTO LRFD Table 12.12.2.4.2-1

Table 1.2 and the above discussion demonstrate that the best backfill materials to allow minimum field control are the Sn soils. There are several classes of these materials:

- crushed rock – crushed rock is created by crushing cobbles and boulders into smaller angular particles. Crushed rock backfills may be uniform (particles fall into a small size range) or graded, and typically have less than 5% fines. Crushed rock backfill generally provides adequate stiffness when dumped and excellent stiffness when subjected to only minimal compaction. Crushed rock generally performs better than the Sn soils, but no suitable data is available to quantify this, it is generally designed as Sn soil. Crushed rock is typically open-graded, and thus steps must be taken to prevent migration of fines if placed next to fine sands and silts.
- pea gravel – pea gravel is the generic name for rounded, uniformly sized stone. Pea gravel flows well into the haunch zone under the pipe and achieves better stiffness than crushed stone when both materials are dumped, but is not as stiff as crushed stone when both materials are compacted. Pea gravel is open-graded, and thus steps, such as the use of a geotextile fabric must be taken to prevent migration of fines if placed next to fine sands and silts.
- sands and gravels – Sands and gravels without fines achieve good densities when dumped and excellent densities when compacted. If placed, spread and compacted in moderate lift thicknesses, excellent pipe support is assured for all typical installations. Sands and gravels may be well-graded or poorly-graded. Poorly-graded gravels may be susceptible to migration of fines. The only exception to this is uniform fine graded

sands. These materials, sometimes called "dune sand" behave more like silts than sands, can be difficult to compact, and are sensitive to moisture content. Use of these materials is controlled by specifying that a maximum of 50% of the particle sizes may pass the No. 100 sieve and a maximum of 20% may pass the No. 200 sieve. Sands not meeting these criteria should be treated as Si materials.

One alternative to specifying coarse-grained backfill materials is to specify controlled low strength backfill (CLSM, also called flowable fill). CLSM is a low strength concrete mix with excellent flow characteristics. It has been shown to provide good pipe performance (McGrath, et al., 1999), but is often quite expensive. It is not discussed further here, but should be considered for installations where the additional cost can be justified.

In Florida, where crushed rock is often not available, sands and gravels are likely the most appropriate choice for structural backfill that will provide the greatest assurance of good performance. These materials provide excellent pipe performance when placed and compacted and are less sensitive to poor construction practices than other materials. We suggest that the preferred backfill meet the requirements of GW or SW material (ASTM D 2487) or AASHTO A-1 or A-3 (AASHTO M145) and meet the limitation on fine sand content listed above. Concrete sand meets these requirements and is generally readily available. Soils with fines (Soils in the Si group) provide good service when properly placed and compacted, but are more susceptible to problems if construction procedures are not followed.

3.2 Backfill Placement

There are many standards that provide construction procedures for buried pipe installation. The most common standard for thermoplastic pipe is ASTM D 2321. This standard provides excellent guidance on a wide range of issues. Most of the issues discussed in this section apply to all types of pipe.

Installation features of particular note that should be present in Florida specifications include:

- trenches should be sufficiently wide to allow joining pipe and proper placement and compaction of the backfill; this condition is generally met if the minimum trench width is 1.5 times the pipe outside diameter plus 12 in.; the space between the trench wall and

the pipe should not be less than the width of the compaction equipment in use on the project. If the native soils forming the trench wall do not stand without support (this means structural support and does not include support supplied solely for worker safety in trenches), increase the trench width to provide one half diameter width of structural backfill on either side of the pipe.

- bedding under the pipe, for the central one-third of the pipe diameter should be left uncompacted for a depth of 3 in. This will provide a softer cushion to support the pipe and will mitigate the effects of poor haunching,
- material must be worked into the haunch zone of the pipe, this generally cannot be properly accomplished if the pipe is backfilled to the springline on the first lift,
- use of trench boxes in the zone of backfill at the side of the pipe is prohibited unless specific steps are taken to assure that the backfill is not disrupted or left with a void when the trench box is advanced,
- trenches must be free of water when placing and compacting backfill,
- lift thickness must be controlled, especially on larger diameter pipe; while 6 in. lifts are commonly specified, work has been completed to show that 12 in. lifts can produce good results with coarse-grained backfills, provided placement and compaction practices are suitable, and
- inspection of the completed pipe installation, including a deflection check, is imperative. For large projects, it is recommended to conduct a partial inspection after completion of a small portion of the project; this inspection can be used to adjust construction practices if necessary, and will prevent the large-scale problem of discovering a systematic flaw at the end of a project; AASHTO Specifications require thermoplastic pipe diameter to be at least 95% of the nominal diameter at the completion of construction; in addition to deflection, post-construction inspections should evaluate line and grade, joint conditions and evidence of impingement due to rocks or other debris in the backfill close to the pipe.

The structural backfill over the top of the pipe serves both to provide a complete envelope for the pipe, and to protect the pipe from incidental impacts due to rock in the final backfill. AASHTO currently recommends that the structural backfill be continued over the top of the pipe to a depth of 12 in. This practice should be continued.

3.3 Backfill Compaction

As noted in prior sections, backfill material type and the compaction level both contribute to the overall stiffness of the backfill and the support provided to the pipe to prevent deflection. The suggested coarse-grained materials provide good stiffness when dumped and reach excellent stiffness with the application of minimal compactive energy. It may be beneficial to require a minimum number of passes of compaction as well as specifying a minimum density requirement. If the contractor is in the habit of supplying some compaction, then good pipe performance will likely be the result even if the compaction percentage is slightly less than specified. The specified density should not be less than 95% of maximum.

Backfill must be compacted at the springline of all pipes.

3.4 Minimum Cover Depth

Minimum cover under roadways is controlled more by the affect of the pipe on the pavement than by stress or deflection levels in the pipe. Three studies are examined to address this issue.

3.4.1 Phares et al. (1998)

Phares et al. (1998) conducted tests on 36 in. diameter corrugated HDPE pipe with 24 in. of cover. The backfill conditions consisted of:

1. uncompacted native soil at the sides and over the pipe,
2. compacted granular soil at the sides of the pipe (to about 70% of the diameter) and compacted native soil over the pipe, and
3. compacted granular soil at the sides and about 12 in. over the pipe with 12 in of compacted native soil over that.

Tests consisted of loading the pipe with a static load applied using a reaction load frame to a plate of unspecified size. The report notes that bearing failures occurred under the load plate during the loading but do not specify the size of the plate or the load at which bearing failure initiated. The longitudinal strain at failure did not vary significantly, averaging about 0.14% strain at wheel loads varying from 6,900 lb (uncompacted condition) to 17,800 lb (compacted granular material to 12 in. over the pipe). They do not report the nature of the failure as cracking (tension) or buckling (compression). An HS20 live load consists of a 16,000 lb wheel, thus the researchers conclude that the factor of safety is on the order of 1.0 at a depth of 2 ft.

The researchers report results that are inconsistent with load tests on full scale pipe with actual vehicles (see the following review of two additional papers), but the acknowledged bearing failure under the load plate is likely having more impact on the pipe performance than the depth of fill. When the soil fails due to excess bearing stresses, it moves out from under the plate and the plate moves closer to the pipe. In these tests, since a steel plate was used, the stresses under the edge of the plate are likely much higher than at the center, further reducing the bearing capacity. In a highway condition, the tire applies a relatively uniform pressure over the load surface. Since live loads increase as a second order function as the depth of cover is reduced, the load applied to the pipe increases rapidly as the plate moves closer to the top of the pipe. Thus, the reported factor of safety of 1.0 at a depth of 24 in. is likely quite conservative. For the time being, more emphasis should be placed on results of actual vehicular load tests to determine expected performance. Of some concern is the finding of a failure strain of 0.13% under a short term loading, however, the behavior that defines the end point of the tests is not identified. See Section 3.4.4 for more discussion of this.

3.4.2 Arockiasamy et al. (2002)

Arockiasamy et al. (2002) report on tests conducted for FDOT as part of an overall assessment of culvert pipes. Pipes with 36 in. and 48 in. inside diameters were buried at depths of 0.5, 1.0 and 1.5 diameters. Two backfills were used, both classifying as poorly graded sands with silt (SP-SM per ASTM D 2487). These materials would both be considered as Si soils per current AASHTO specifications for thermoplastic pipe. Live loads were calculated based on an HS-20 truck with additional load to account for impact per AASHTO LRFD. For the 0.5 diameter burial case, this was an axle load of approximately 40,000 lb. Changes in vertical diameter were about 0.2 in. maximum for the depth of 0.5 diameter, 36 in. pipe. Maximum measured

longitudinal tensile strains were 0.05% for the same depth. No failures or damages to the pipe were noted.

In simple beam longitudinal tests, the researchers report failure strains on the order of 0.36% to 0.82%. Slightly larger than those reported by Phares but still extremely low. The nature of the pipe behavior at the end of the test is not identified.

The researchers conclude that minimum cover depth below the top of an unpaved road should be no less than 36 in. or one pipe diameter, whichever is smaller based on the measured longitudinal strains of 0.05% and the Phares reported failure strain of 0.14%.

3.4.3 McGrath et al. (2002)

McGrath et al. (2002) provided an interim report on live load testing of 60 in. diameter pipe under depths of fill of 1 and 2 ft over a period of two years. A total of 8 HDPE pipes were installed, along with one concrete and one corrugated steel pipe that were used as references. The study used two backfill materials, a coarse-grained material without fines and a silty sand with about 25% fines. Both backfill materials were compacted to 90% of maximum. The pipes were installed in the Minnesota Research Road facility, a closed loop road that is subjected to repetitive cycles of truck loads with axle loads of 18,000 and 24,000 lbs. The peak circumferential tensile strains recorded during live load testing were approximately 0.12% at 1 ft of cover. Peak deflections under live load were on the order of 0.12 in. In the cited paper, there was some concern that the deflections were increasing with time; however, continued observation (not yet published) did not bear this out. The deflections increase slightly during the spring thaw but then return to lower values. The overall pipe deflections have been stable for the 2 year life of the project. The testing work is being used to calibrate full three-dimensional pipe-soil models of the live load condition, and the models are then being extended to evaluate design axle loads with impact. These studies, while not published suggest good pipe behavior at a depth of 2 ft.

The Minnesota test did show that the thermal expansion and contraction of the pipe during seasonal changes are significant. The thermal expansion of polyethylene is approximately 10 times that of steel, and, since the backfill at the sides of the pipes is stiff, all of the thermal expansion and contraction is seen as up and down motion of the crown. This led to low spots developing in the roadway during the winter months when the pipe contracted, and also led to

cracking in the pavement over the pipes. The cracking was significantly reduced for the two foot depth of cover condition relative to the one foot depth of cover condition. There was some cracking over the crown of the metal pipe and none over the crown of the concrete pipe. Although not final at this time, the researchers are anticipating recommending a minimum cover limit of 2 ft or 0.5 diameters, whichever is greater.

3.4.4 Discussion

Overall, the minimum depth of cover recommended by Arockiasamy et al. (2002) seems to depend mostly on the low longitudinal strengths from their own simple beam tests and those reported by Phares et al. (1998). The reported failure strains suggests a stress on the order of a few hundred psi, which is much lower than strengths reported by Dr. Hsuan in this study for tests on the intersection of the liner and corrugation, which is likely the weakest part of the profile. Neither researcher reports if the failures were due to tensile cracking or compressive buckling, but it is likely that the end point of the tests is the result of a compressive buckling in the pipe wall, a behavior that would be restrained in buried pipe. The reported failure strains from the simple beam tests should not be considered a material limit. Overall, this suggests that The recommended minimum depth of cover of 36 in. or one pipe diameter, whichever is less proposed by Arockiasamy et al. (2002) may be unnecessarily conservative.

At the current time, the minimum depth recommendation from the Minnesota study is recommended as a suitable control to provide good service for unpaved roads. Recommended minimum depths of cover in a format consistent with current Florida specification formats are presented in Table 1.3

Table 1.3 – Recommended Minimum Depth of Cover (in.)

Pipe Diameter	Rigid Pavement Depth below bottom of pavement, in.	Flexible Pavement Depth below bottom of base, in.	No Pavement	
			Commercial	Non-Commercial
up to 48 in.	9	15	24	12
54 in., 60 in	15	21	30	24

For unpaved roads, non-commercial traffic is considered to include applications such as driveway culverts where the typical vehicular traffic does not any include trucks, thus, loading with a vehicle such as an HS-20 truck would be rare. Installation quality, backfill material and backfill compaction are still considered to meet the standards set for other applications.

4. CONCLUSIONS

Florida DOT initiated a study to determine requirements for assuring that corrugated HDPE pipe will provide a 100 year service life. The study was initiated at Drexel University and at Simpson Gumpertz & Heger Inc. Drexel University has prepared a separate report on material strength characteristics that are required to assure good material performance. This is Part II of the current report. This Part I report presented the results of the Simpson Gumpertz & Heger Inc. study to evaluate the anticipated stress levels that a pipe installed for 100 years would be subjected to, and recommendations for backfill materials and construction procedures to control stresses. Recommended design and installation procedures are presented in AASHTO format as an attachment to this report.

This Part I study consisted of a parametric analysis of expected performance of buried corrugated HDPE pipe under earth loads with several compaction conditions, varying depths of fill, and variable support under the pipe haunches. This study demonstrates that tensile stresses are relatively low when pipe installation meets typical requirements and maintain changes in vertical diameter to less than 5%. Long-term tensile strain for the service condition should be less than 1.6%, corresponding to a long-term stress of approximately 300 psi, or about 2.5% and 500 psi for the factored load condition. This is significantly reduced from the current AASHTO requirement of 5% long-term tensile strain capacity. Review of a study on three-dimensional analysis of longitudinal strains, and consideration of poor grade control of pipe during installation indicates that this recommended minimum stress level should also apply

to longitudinal stresses. In both cases, the limiting stress condition applies to the general field stresses, and is not associated with areas of stress concentration, such as the intersection of the liner and corrugation.

Backfill materials that provide the best performance with minimal controls on construction procedures are well-graded coarse-grained soils (sands and gravels, GW and SW per ASTM D 2487) with less than 12% fines. Uniformly graded coarse-grained soils (GP and SP per ASTM D 2487) also provide good service but are not recommended unless provisions are made to evaluate and control possible migration of fines into open voids. Uniform fine sands should be avoided and criteria were presented for controlling this. Coarse-grained soils with fines (GC, GM, SP, SM, or AASHTO A-2-4 or A-2-5) or fine grained soils with at least 30% coarse grained material (sandy silts and sandy clays) provide good service if placed and compacted properly, but increased inspection during construction is recommended. Backfill should be compacted to at least 95% of maximum standard Proctor density.

The most important aspect of construction control is to inspect corrugated PE pipe after installation, including the measuring of vertical diameters. Total reduction in vertical diameter should be limited to 5%. On large projects deflections should be evaluated after a small portion of the project has been completed to determine if the construction procedures are adequate.

Suggested minimum cover depths for applications subjected to live loads are based on the findings of the Minnesota study. The minimum depth of fill should be the larger of 2 ft or one-half of the pipe diameter. Specific recommendations consistent with Florida specifications were presented.

5. REFERENCES

AASHTO (1998a). *AASHTO LRFD Bridge Design Specifications 2nd Edition with Interim Specifications through 2002*, American Association of Highway and Transportation Engineers, Washington, DC.

AASHTO (1998b). *AASHTO LRFD Bridge Construction Specifications 1st Edition with Interim Specifications through 2002*, American Association of Highway and Transportation Engineers, Washington, DC.

Arockiasamy, et al. (2002). Arockiasamy, M., Chaallal, O., Limpeteepakarn, T., and Wang, N., *Experimental and Analytical Evaluation of Flexible Pipes for Culverts and Storm Sewers, Volume II Laboratory Work and Numerical Analysis*, Florida Atlantic University, Boca Raton, FL.

Arockiasamy, et al. (2002). Arockiasamy, M., Chaallal, O., Limpeteepakarn, T., and Wang, N., *Experimental and Analytical Evaluation of Flexible Pipes for Culverts and Storm Sewers, Volume III Field and Experimental Work and Numerical Analysis*, Florida Atlantic University, Boca Raton, FL.

Arockiasamy, et al. (2002). Arockiasamy, M., Chaallal, O., Limpeteepakarn, T., and Wang, N., *Experimental and Analytical Evaluation of Flexible Pipes for Culverts and Storm Sewers, Volume IV Parametric Studies, Analyses and Recommendations*, Florida Atlantic University, Boca Raton, FL.

Chambers et al. (1980). Chambers, R.E., McGrath, T.J., and Heger, F.J., *Plastic Pipe for Subsurface Drainage of Transportation Facilities, NCHRP Report 225*, Transportation Research Board, National Research Council, Washington, DC.

Chambers and McGrath (1981). Chambers, R.E., and McGrath, T.J., "Structural Design of Buried Plastic Pipe," *Proceedings of the International Conference on Underground Plastic Pipe*, ASCE, New Orleans, LA.

Duncan et al. (1980). Duncan, J.M., Byrne, P., Wong, K.S., and Mabry, P., "Strength, Stress-strain and Bulk Modulus Parameters for Finite Element Analysis of Stresses and Movements in Soil Masses," *Report No. UCB/GT/80-01*, University of California, College of Engineering, Berkeley, California, August, 1980.

Howard, A. (1996). *Pipeline Installation*, Relativity Publishing, Lakewood, CO.

Hsuan and McGrath (1999). Hsuan, Y.G., and McGrath, T.J., "HDPE Pipe: Recommended Material Specifications and Design Requirements," *NCHRP Report 429*, Transportation Research Board, National Research Council, Washington, DC.

McGrath, et al. (1990). McGrath, T.J. Chambers, R.E., Sharff, P.A., "Recent Trends in Installation Standards for Plastic Pipe," *Buried Plastic Pipe Technology, ASTM STP 1093*, George S. Buczala and Michael J. Cassady, Eds., American Society for Testing and Materials, Philadelphia, PA, 1990.

McGrath (1999). McGrath, T.J., "Calculating Loads on Buried Culverts Based on Pipe Hoop Stiffness," *Transportation Research Record, No. 1656*, The Transportation Research Board, Washington, DC.

McGrath, et al. (1999). McGrath, T.J., Selig, E.T., Webb, M.C., and Zoladz, G.V., "Pipe Interaction with the Backfill Envelope," *Publication No. FHWA-RD-98-191*, U.S. Department of Transportation Federal Highway Administration, McLean, VA.

McGrath et al. (2002). McGrath, T.J., DelloRusso, S.J., and Boynton, J., "Performance of Thermoplastic Culvert Pipe Under Highway Vehicle Loading," *Pipelines 2002*, G. Kurz Ed., American Society of Civil Engineers.

Moore, I.D. (1995). "Three-Dimensional Response of Deeply Buried Profiled Polyethylene Pipe," *Transportation Research Record, No. 1514*, The Transportation Research Board, Washington, DC.

Moore, I.D. and Hu, F. (1995). "Response of Profiled High-Density Polyethylene Pipe in Hoop Compression," *Transportation Research Record, No. 1514*, The Transportation Research Board, Washington, DC.

Phares, B.M., Wipf, T.J., Klaiber, F.W., and Lohnes, R.A., (1998). "Behavior of High-Density Polyethylene Pipe with Shallow Cover," *Transportation Research Record, No. 1624*, The Transportation Research Board, Washington, DC.

Selig, E.T. (1988). Soil Parameters for Design of Buried Pipelines, *Pipeline Infrastructure — Proceedings of the Conference*, American Society of Civil Engineers, New York, NY, pp. 99-116.

PART II - Stress Crack Resistance, Oxidation Resistance and
Viscoelastic Properties of Corrugated HDPE Pipes

1. INTRODUCTION

This Part II of the report, is entitled “Protocol for Predicting Long-term Service of Corrugated High Density Polyethylene Pipes”. This part of the report consists of three topics: stress crack resistance of corrugated HDPE pipes, antioxidant formulation in the pipe to ensure oxidation stabilization, and long term tensile and flexural modulus properties.

A series of laboratory tests were performed to assess the various issues in the three focused areas of the project to establish specification requirements for long-term service life of corrugated HDPE pipes for potential use on Florida DOT projects. The intention of these laboratory tests is also to verify the test methods that are incorporated in this test protocol, as well as to illustrate the test procedures and analyses. Due to the limited number of pipe samples being evaluated in this project, the test data may not represent the behavior of all corrugated HDPE pipes. Furthermore, some of the tests require a much longer testing time than was the duration of the project. Thus, the preliminary test values presented in the report may not reflect the long-term performance of the pipes.

2. TEST MATERIALS

Two 24 in. and one 36 in. diameter corrugated HDPE pipes were supplied by two manufacturers for the laboratory study. These pipes are coded as P-1, P-2 and P-3. Table 2.1 shows the properties of the three pipes according to methods listed in AASHTO M 294. The tests were performed on the compression plaques that were prepared by remolding the cut pipe pieces. The HDPE resins are not available for the evaluation. Thus, material properties in Table 1 cannot be directly compared with those required in M 294 which refers to opaque non-carbon black resin material. Also the oxidative induction time (OIT) test data was included to characterize the antioxidant amount in the pipes.

Table 2.1 – Properties of P-1, P-2 and P-3 Pipes

Properties	P-1	P-2	P-3
Diameter (in.)	24	24	36
Density (g/cc)	0.953 ⁽¹⁾	0.951 ⁽¹⁾	0.951 ⁽¹⁾
Melt Index (g/10min)	0.16	0.25	0.28
Flexural modulus (psi)	124,400	117,700	na
Tensile strength (psi)	4040	3700	na
Carbon black (%) (minimum)	2.6	2.6	2.5
NCLS* test (hours)	17.8	19.8	34.6
OIT ⁺ test (minutes)	26.4	30.6	44.6

* NCLS test – Notched constant ligament stress test

+ OIT test – Oxidative induction time test

(1) The density values were obtained by calculation using equation in ASTM D 3350.

(2) na – not available

3. LABORATORY TESTS TO EVALUATE LONG TERM STRESS CRACK RESISTANCE OF CORRUGATED HDPE PIPES

3.1 Background

The material specification for corrugated HDPE pipes used in transportation applications is based on AASHTO M294 “Standard Specification for Corrugated Polyethylene Pipes”. In the year 2002, the specification adopted the NCLS test which is now ASTM F2136 “Standard Test Method for Notched Constant Ligament Stress (NCLS) Test to Determine Slow Crack Growth Resistance of HDPE Resins or HDPE Corrugated Pipe”. The modification enhances the SCR of HDPE resins used for corrugated pipes. The NCLS test is a constant stress test in which stress relaxation does not developed, thereby presenting a greater challenge to SCR of the test specimens in comparison to constant strain test (i.e., ASTM 1693) which was required by the specification until 1999. The minimum cell classes defined in AASHTO M294 are shown in Table 2.2 together with the specified property ranges within each of the cell classes.

In the current M294 specification, environmental stress crack resistance (ESCR) and hydrostatic design basis (HDB) tests, are not specified; instead the NCLS test is required in the specification. Resin samples are made from plaques according to ASTM D 4703. The conditions of the NCLS test are defined to be at 50°C in a 10% Igepal[®] solution under an

applied stress of 600 psi. The average failure time of five test specimens must be greater than 24 hours and no single specimen failure shall be less than 17 hours.

Table 2.2 – Cell Class Properties for Corrugated HDPE Pipes

Properties	Cell Class	Value
Density	3	< 0.945 – 0.955 g/cc
Melt Index	3	< 0.4 – 0.15 g/10 min
Flexural modulus	5	110,000 to <160,000 psi
Tensile Strength	4	3,000 - <3,500 psi
ESCR*	0	unspecified
HDB ⁺	0	unspecified
UV stabilizer	C	2% minimum carbon black

* ESCR – Environmental stress crack resistance

⁺ HDB – Hydrostatic design basis.

For finished pipe test, the M-294 specification retained the 90° pipe bending test for the evaluation of SCR on the finished pipes. This bending test is based on the same stress condition as ASTM D1693. The pipe section is under a constant strain condition, thereby allowing stress relaxation to take place during the testing. This finished pipe test does not appropriately challenge the SCR properties of the pipe. Furthermore, the test is impractical for large diameter pipes. Most important, however, the test does not challenge the specific locations that are sensitive to stress cracking, such as junctions, longitudinal profiles, and processing defects. Alternative SCR tests on the finished pipe were developed in this study and are incorporated into the test protocol for predicting long-term stress crack resistance of the finished pipe. The new SCR tests are applied to both short and long-term evaluations. The short-term tests are used for quality assurance and quality control (QA/QC) purposes to confirm the properties of pipes that have previously demonstrated 100-year crack free performance by manufacturers or users. The long-term evaluation employed tests that are performed under a range of different environmental conditions for long-term prediction purpose.

3.2 Stress Crack Resistance of Corrugated HDPE Pipes

In the current M294, the NCLS test focuses on plaque made of pipe resin; thus, the effects of the pipe manufacturing processes are not evaluated. Since corrugated pipes have a complex

geometric profile, some parts of the pipe are more susceptible to stress cracking due to high stress concentrations than others. The protocol in this study utilizes three SCR tests to evaluate different parts of the corrugated pipe. The test specimens are taken directly from the pipe so that the manufacturing process and design effects can be challenged.

3.2.1 Stress Crack Resistance of the Corrugated Pipe Liner

NCHRP Report 429-Table 6 shows that the majority of field cracked pipes exhibited circumferential cracking that took place in the liner adjacent to the junction between liner and corrugation of the pipe, as shown in Fig. 2.1. Moore (1995) utilized three-dimensional finite element analyses to examine the stress distribution in corrugated pipe under different burial conditions and found that an axial tension existed in the liner near the junction region. Therefore, the pipe liner is a critical component regarding crack free service life evaluation.

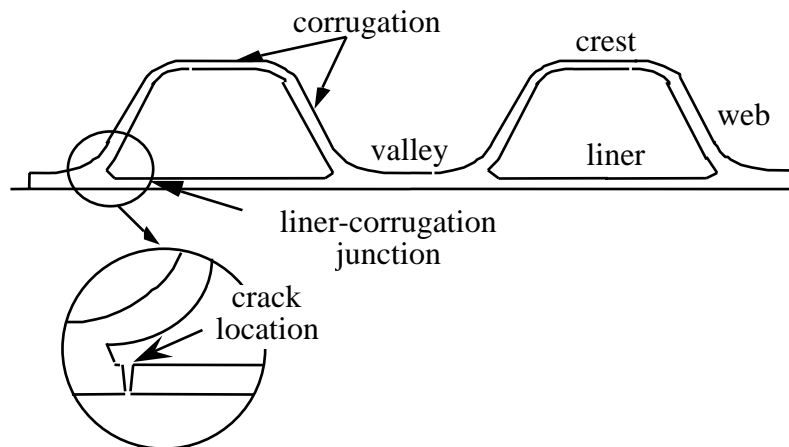


Fig. 2.1 – Schematic diagram illustrating the location of circumferential cracking in corrugated HDPE pipes.

The NCLS test was used to evaluate the SCR of pipe liner. However, test specimens were taken directly from the pipe liner, as shown in Fig. 2.2(a). A 20% notch depth was introduced to the specimen on the outer side of the liner, Fig. 2.2(b). The test procedure is described in the Florida Method of Test FM 5-572 – Procedure A. Table 2.3 shows the summary of results for the three pipes that were used to assess the method. The test data indicate that two of the pipes exhibit noticeably different SCR properties between the liner and compression molded plaque. Such difference is caused by the manufacturing process effects which exist in the pipe liner but not the plaque. An extensive study on the effect of manufacturing process was carried

out in the NCHRP 4-26 project. The reduction factors (ratio of failure time of pipe liner versus pipe plaque) of 24 tested pipes were in the range of 0.44 to 0.91.

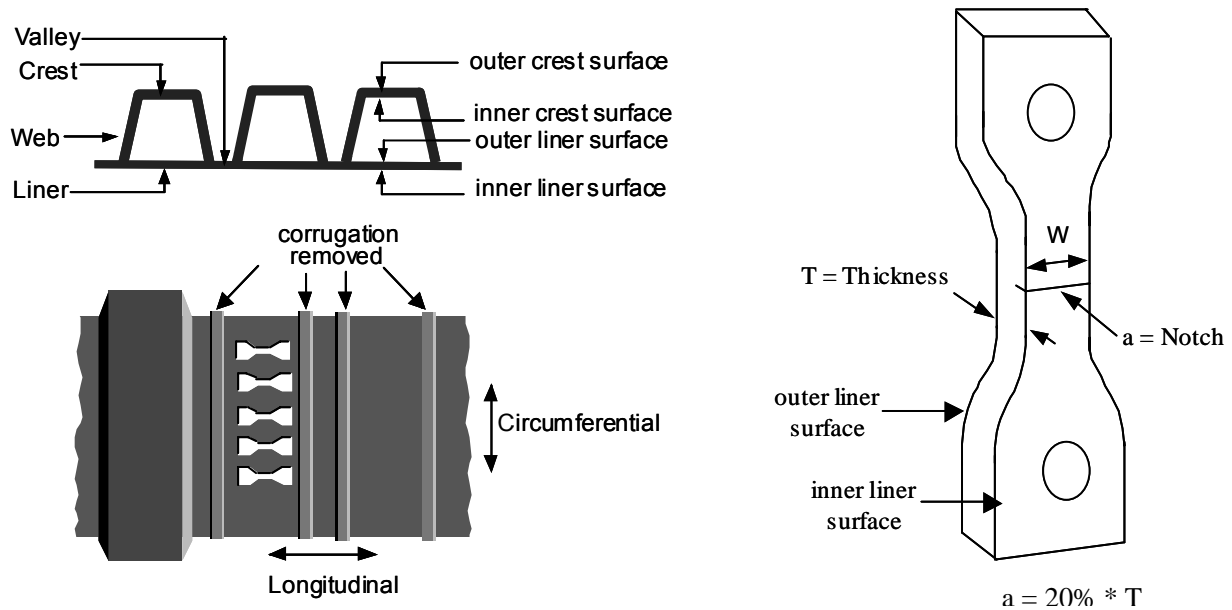


Fig. 2.2 Location of the test specimens taken from the pipe liner and notch location on the specimen

Table 2.3 – Results of NCLS Test of Pipes P-1, P-2, and P-3

Pipe	Average Failure Time of Molded Plaque (hr)	Average Failure Time of Pipe Liner (longitudinal) (hr)	Failure Time Ratio (pipe/plaque)
P-1	17.8	12.6	0.71
P-2	19.8	19.5	0.98
P-3	34.6	24.5	0.71

In addition, the ductile-to-brittle curves of three pipe liners were established, as shown in Fig. 2.3. The slopes of the ductile and brittle curves of the three pipes are very similar, as shown in Table 2.4. However, the slopes of the brittle curves are steeper than those reported in the NCHRP Report 429 in which the brittle slopes obtained from compression molded plaques were found in the range of 0.24 to 0.44. The steep brittle slope resulting from the pipe liner may again be caused by the effects of the manufacturing process which tends to decrease the SCR of the corresponding resin.

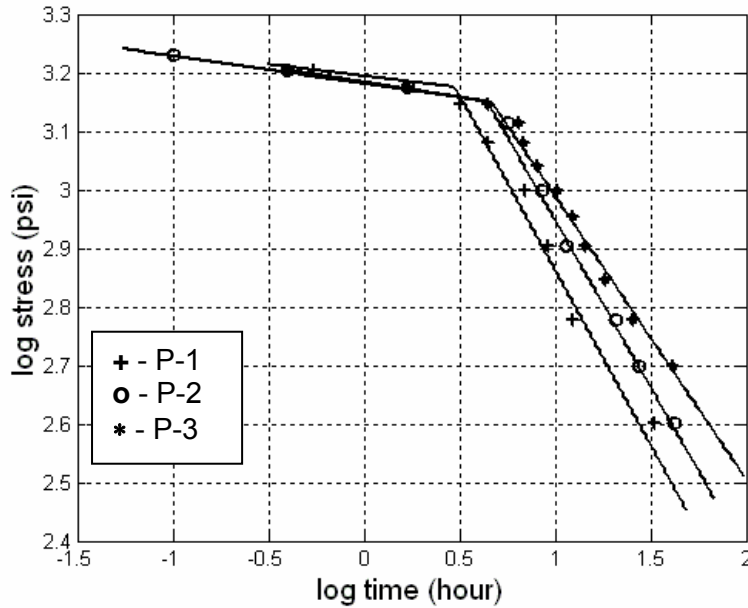


Fig. 2.3 – Ductile-Brittle curves of three tested pipes, P-1, P-2 and P-3

Table 2.4 – Slope Values of Ductile and Brittle Regions from Fig. 2.3

Pipe	Ductile	Brittle
P-1	-0.0396	-0.5962
P-2	-0.0471	-0.5703
P-3	-0.0511	-0.4842

3.2.2 Stress Crack Resistance of the Liner/Corrugation Junction

As shown in Fig. 2.1, the junction between the liner and corrugation is susceptible to stress cracking due to abrupt changes in the geometry. The junction geometry is governed by the pipe design as well as the extrusion process. If an axial tensile stress is imposed across the junction, as indicated by Moore (1996), cracking could occur under this complex mechanism

A new SCR test on the junction was developed based on the preliminary work that was reported in NCHRP Report 429. The test procedure to evaluate the liner/corrugation junction is described in the Florida Method of Test FM 5-572 – Procedure B. The ASTM D 638 Type IV die size has been adopted in this test. Depending on the width of the pipe valley, two sides of the junction can be evaluated simultaneously or separately, as shown in Figs. 2.4 and 2.5, respectively.

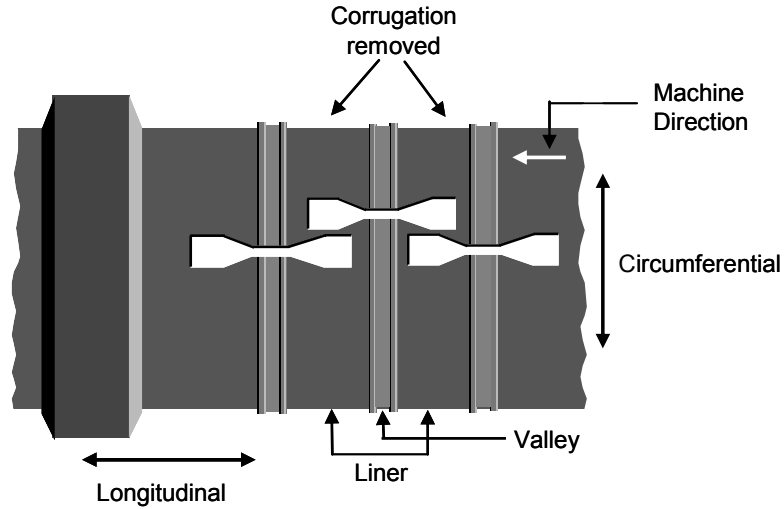


Fig. 2.4 – Locations of SCR junction specimens taken from junction width less than 1.0 inch

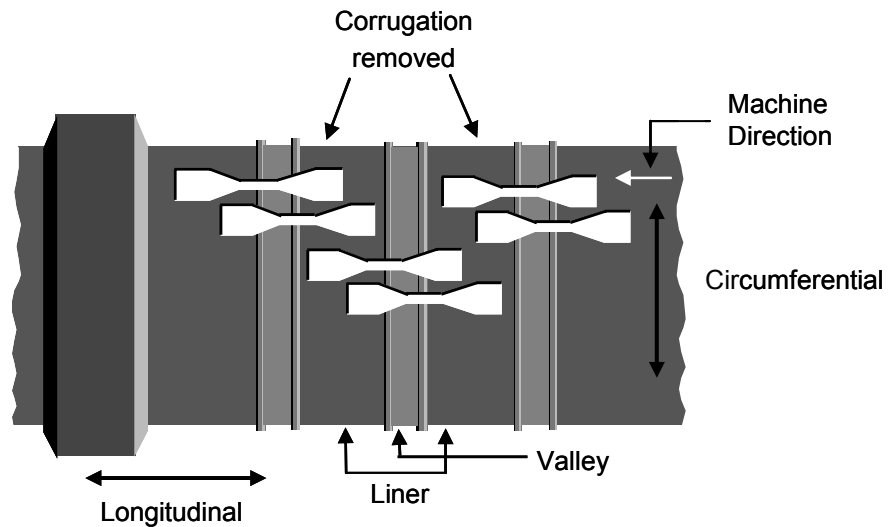


Fig. 2.5 – Locations of SCR junction specimens taken from junction width greater than 1.0 inch

The pipe junction tests were performed in test conditions similar to those in the NCLS test namely, 10% Igepal solution at 50°C under applied stress of 600 psi. Both P-1 and P-2 pipes were evaluated. The results are shown in Table 2.5. They indicate the vulnerability of the junction or adjacent areas towards stress cracking. For the P-1 pipe, the failure of the junction-specimen was not at the junction. The cracking actually started from the inner liner and then continued through the valley part of the pipe, as shown in Fig. 2.6. In P-2, the geometry of the junction clearly governed failure. One side of the junction exhibited much greater crack

resistance than the other. The failure took place at the junction between liner and corrugation, as shown in Fig. 2.7.

Table 2.5 – Results of Junction Tests on Pipes P-1 and P-2

Pipe	Failure Time (hr)	Comments
P-1 both sides	207 1238	Two out of five specimens failed. Failure occurs at the inner liner first and then grows through the material. (Three specimens are still on-going after 1500 hr.)
P-2 Side one	62	All seven specimens failed with standard deviation value of ± 28 hr.
P-2 Side two	882 1120 1030	Three out of four specimens failed. (One specimen is still on-going after 1500 hr.)

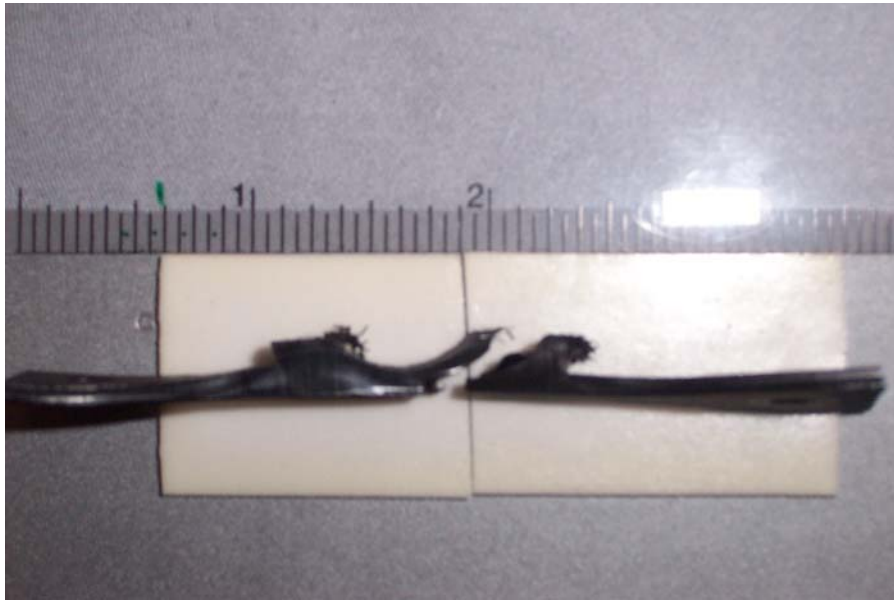


Fig. 2.6 – Failure of junction-specimen from pipe P-1



Fig. 2.7 – Failure of junction-specimen from pipe P-2

3.2.3 Stress Crack Resistance of Longitudinal Profiles

NCHRP Report 429-Table 6 shows that in some of the field cases, longitudinal cracking was observed in the corrugated pipe. Some of the longitudinal cracks were noted to be along the vent hole or mold line of the annular profile pipes. Vent hole and molded line cracking was observed in Site J of the NCHRP Report 429 (note that the vent hole photos were not included in the report.) Furthermore, one of the PIs of this project has extensive experience in field performance of the corrugated pipes, and he has observed vent hole cracking in the field. Thus, these locations shall be evaluated to ensure long-term crack free performance of the pipe.

A new SCR test was developed for this assessment. The test procedure to evaluate the longitudinal profiles is described in Florida Method of Test FM 5-572 – Procedure C. The ASTM D 638 Type IV die size was adopted in this test. The specific profile that is tested is positioned at the center of the constant neck section of the specimen, as shown in Fig 2.8.

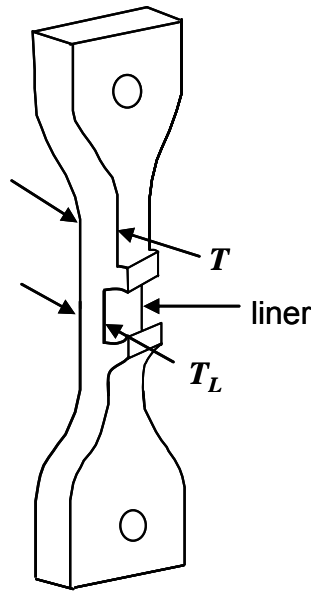


Fig. 2.8 – Specimen configuration for vent hole location

In this study, the selected longitudinal profile was a vent hole so as to illustrate the test method. The test was performed in 10% Igepal solution at 50°C under an applied stress of 600 psi. Table 2.6 shows the test results which indicate that cracking at longitudinal profiles (in this case, the vent holes) is possible. Of significance is that the failure resulting from this test appeared very similar to those observed in the field. Fig. 2.9 shows a failed specimen. Cracking started from the inner liner and then progressed through the crown of the vent hole.

Table 2.6 – Results of Longitudinal Profile Tests at Vent Holes

Specimen No.	Failure Time (hr)	Comments
1	176	Three out of five specimens failed. Failure started from the inner liner and then the crown. The other two specimens are still on-going after 1200 hr.
2	784	
3	856	

Note: this set of tests was performed under applied stress of 500 psi due to equipment limitations. The actual test should be performed at 600 psi



Fig. 2.9 – Failed longitudinal profile (vent hole) specimen

However, the test data in Table 2.6 resulted from applied loads that were calculated based on the valley thickness of the pipe. In addition, the bending stress that was induced due to straightening of the specimen was not removed from the applied load. Since test specimens were taken from the circumferential direction of the pipe, they consist of a curvature that varies with the diameter of the pipe. The smaller pipe diameter creates a greater curvature in the test specimen. Under a constant tensile test configuration, the curved test specimen was forced to be straightened; thus, induced tensile stress on the liner part of the vent hole. Without considering this induced tensile stress, the liner portion of the specimen was subjected to a stress higher than the test intended. In the newly developed Florida test method, the induced stress due to the straightening of the test specimen was subtracted from the applied load. Also the thickness of the liner was used to calculate the applied load instead of the valley thickness. Since the failure started at the liner of the vent hole, the upper part of the vent hole is removed or cut, so that the applied load is transmitted through the liner only.

3.3 Long-Term Stress Crack Resistance of Pipes

The three tests described in Section 3.2 are intended to be used for manufacturing QA/QC purposes. As such, the test environment is intended to accelerate failure mechanisms so that tests can be completed in a relatively short period of time. The test results do not directly reflect the long-term performance of the pipe unless a correlation is established over a period of time.

That said, the manufacturing QA/QC tests are critical in validating the quality of the finished pipe.

Regarding the long-term crack resistance (100-year design life) of corrugated HDPE pipes, there are inadequate long-term performance case histories available for pipes made from the newly adopted resins. Thus, accelerated laboratory tests should be used for the long-term performance prediction. The environment of such acceleration tests should be as close to field conditions as possible. In this regard, the liner of the drainage pipes is exposed to two media; water and air. Therefore, these two environments will be used in the tests for predicting the long-term performance.

3.3.1 Test Environments

The conditions of the NCLS test have been modified by using water and air as test media instead of a 10% Igepal solution. In addition, the NCLS test was performed at three elevated temperatures to observe the temperature acceleration effect.

3.3.1.1 Water Environment

The NCLT tests using water as the test medium were performed on the liner part of P-3 pipe at test temperatures of 60, 70 and 80°C and applied stresses from 300 to 1600 psi. Note that due to the large number of tests; only three specimens were tested at each stress level. Fig. 2.10 shows the log stress versus log failure time plots at three temperatures. The slopes and the ductile-to-brittle transition points of the curves at these three temperatures are given in Table 2.7. Note that the slopes of brittle curves are relatively similar to each other.

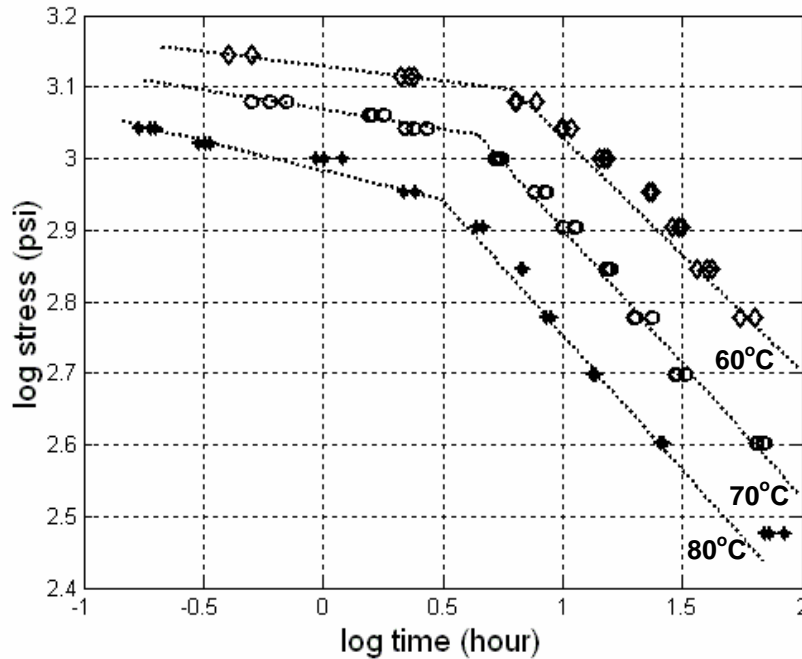


Fig. 2.10 – Applied stress versus failure time curves of P-3 in water

Table 2.7 – Information Obtained from Ductile-to-Brittle Curves in Water

Environment	Temperature (°C)	Transition Point		Slope	
		Stress (psi)	Time (hr)	Ductile Region	Brittle Region
Water	60	1248	6.3	0.041	0.33
	70	1077	4.5	0.055	0.38
	80	875	3.2	0.082	0.38

3.3.1.2 Air Environment

The NCTL test in air was performed on the liner part of the P-3 pipe at temperatures of 60, 70 and 80°C in a forced air oven. The applied stresses ranged from 300 to 1600 psi. Note that due to the large number of tests; only three specimens were tested at each stress level. Fig. 2.11 shows the log stress versus log failure time plot at three temperatures. The slopes and the ductile-to-brittle transition point of the curves at these three temperatures are given in Table 2.8. The slope of the brittle region at 60°C is slightly lower than those at the higher temperatures.

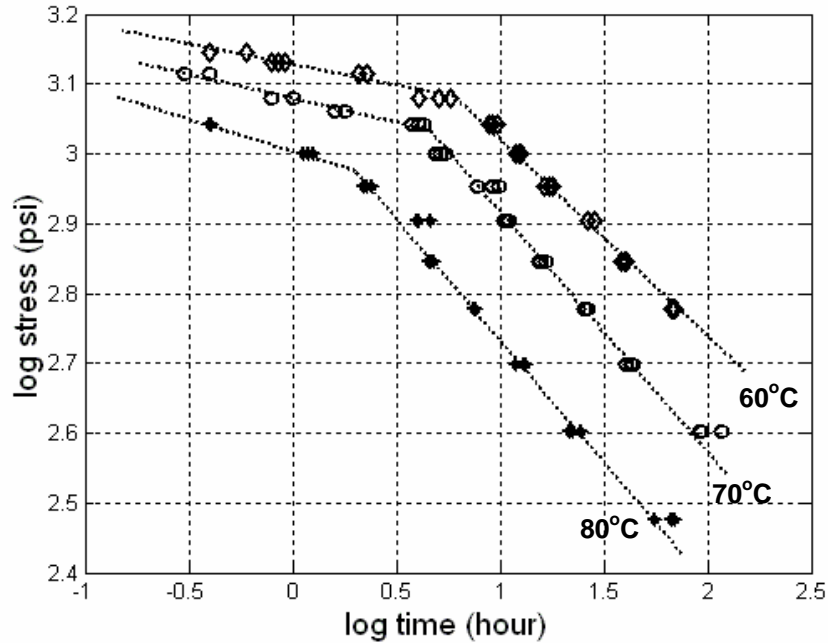


Fig. 2.11 – Applied stress versus failure time curves of P-3 in air

Table 2.8 – Information Obtained from Ductile-to-Brittle Curves in Air

Environment	Temperature (°C)	Transition Point		Slope	
		Stress (psi)	Time (hr)	Ductile Region	Brittle Region
Air	60	1206	6.1	0.059	0.28
	70	1081	4.5	0.082	0.36
	80	944	2.0	0.092	0.35

By comparing test data obtained from water and air environments, their failure times are relatively similar. In the NCHRP Report 429, the results of the field investigation indicate that the circumferential cracking took place in both wet and dry regions (i.e., invert and crown regions) of the pipe. Based on the field observations and the application function of the pipes, testing in a water environment seems to be appropriate in simulating field conditions. In addition, a uniform testing temperature can be achieved easier in water than in air.

It should be noted that the NCLS test uses notched specimens. The purpose of the notch is to shorten the time for crack to form by creating a high stress concentration at the tip of the notch, thereby generating a consistent failure time under the same test parameters. Although the probability for pipes to have defects with similar stress concentration as the notch is largely

unknown, the pipe does contain many stress concentration locations, such as the junction between liner and corrugation and different types of longitudinal profiles. A performance test that challenges those stress concentration locations will be presented in Section 3.3.2 of this report.

3.3.1.3 Comparing Different Test Environments

In Fig. 2.12, the ductile-to-brittle curves from three test environments at 50°C are compared. Readily seen is that at the same test temperature, the 10% Igepal solution provides the greatest acceleration effect on stress cracking. The failure times at all stress levels are significantly shortened and the transition stress is slightly higher than those in water and air. The slope of the brittle curve in 10% Igepal solution is much steeper, with a value of 0.5, in comparison to 0.34 and 0.31 for water and air, respectively. At the applied stress of 600 psi, the failure time is seven times faster in 10% Igepal solution than in water and air. As noted previously, the responses between water and air are similar to one another.

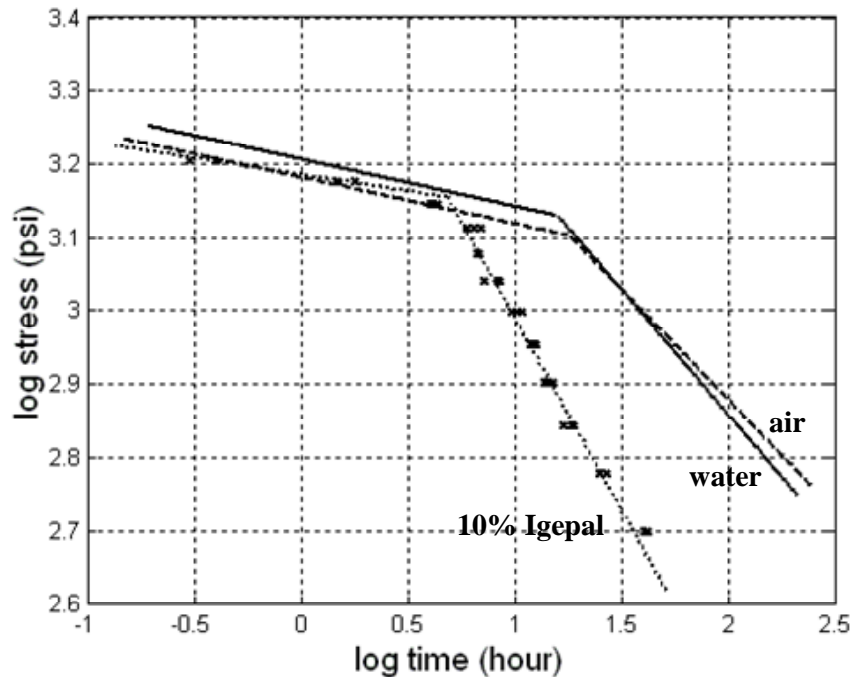


Fig. 2.12 – Ductile-to-brittle curves in three different test environments at 50°C

3.3.2 Performance Test for Assessing SCR of Corrugated HDPE Pipes

In Sections 3.2.2 and 3.2.3, the susceptibility of the pipe junction and longitudinal profiles were demonstrated using test conditions of 10% Igepal at 50°C under an applied stress of 600 psi. While such test conditions are appropriate for an acceleration test, they are not suitable for predicting the long-term SCR. In this section, the results of tests on pipe junctions using a water environment at temperatures of 60, 70 and 80°C under applied stress ranging from 350 to 1000 psi are presented. The junction specimens were removed from P-1; a 24-in pipe. The configuration of the test specimen is according to Fig. 2.4 in which two junctions were tested simultaneously in one specimen.

Fig. 2.13 shows the log stress versus log failure time response of the junction tests. The properties of the ductile-to-brittle curves are given in Table 2.9. As expected, the failure times of the junction specimens are much longer than those of the notched liner specimens, since the stress concentration is lower at the junction than at the notch tip. Also the slope of the brittle line is lower in the junction test than the notched liner test.

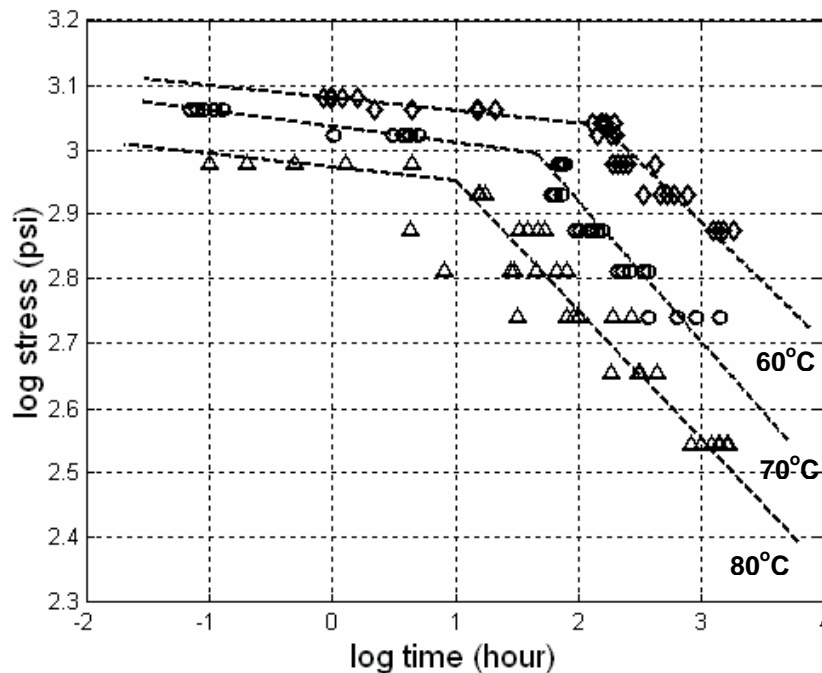


Fig. 2.13 – Applied stress versus failure time curves for junction tests of P-1

Table 2.9 – Properties Obtained from the Ductile-to-Brittle Curves in Fig. 2.13

Temperature (°C)	Transition time (hour)	Transition stress (psi)	Slope in brittle region	Slope in ductile region	Constants in brittle region	Constants in ductile region
60	158	1088	-0.1855	-0.0195	A = -25.11	A = -82.39
70	46	987	-0.2174	-0.0250	B = 14295	B = 68098
80	9.6	942	-0.1785	-0.0227	C = -1717	C = -13132

3.3.3 Prediction Methods

Three methods have been investigated in the prediction of stress crack resistance of the corrugated HDPE pipes, and they are ISO 9080, Popelar Shift Method (PSM) and Rate Processing Method (RPM).

3.3.3.1 ISO 9080 Standard

ISO 9080 describes the methodology to determine the ductile-to-brittle transition point and the best fitted lines for ductile and brittle regions. In addition, the standard utilizes the Arrhenius Equation, Eq. 2.1, with an activation energy of 110 kJ/mol to generate a series of factors for failure time extrapolation from high testing temperature to low site temperature.

$$t = Ae^{\frac{E}{RT}} \quad \text{Eq. 2.1}$$

Where:

- t = failure time (hour)
- E = activation energy (kJ/mol)
- R = gas constant (8.14 J/mol)
- T = absolute temperature (K)
- A = constant

By adopting the Arrhenius Equation, it is assumed that the ductile-to-brittle curves at different temperatures are parallel to each other. However, this has found to be not rigorously true. The slope of the curves changes with temperature, particularly at lower temperatures. Furthermore, the method does not provide an adjustment for the effect of temperature on the applied stress.

3.3.3.2 Popelar Shift Method (PSM)

Based on many sets of ductile-to-brittle curves, Popelar, et al. (1990) developed two (constant) shift factors to shift individual data points in both time and stress, as expressed in Eqs. 2.2 and 2.3, respectively.

$$a_T = \exp[-0.109(T - T_R)] \quad \text{Eq. 2.2}$$

$$b_T = \exp[0.0116(T - T_R)] \quad \text{Eq. 2.3}$$

where:

- a_T = horizontal shift function (time function)
- b_T = vertical shift function (stress function)
- T = temperature of the test
- T_R = target temperature

The accuracy of these two shift factors has not yet verified for corrugated HDPE pipes.

3.3.3.3 Rate Processing Method (RPM)

RPM has been used to analyze stress crack test data of HDPE pressured pipe materials for many years and it is included in both ISO 9080 and ASTM D 2837. The general equation of RPM is expressed in Eq. 2.4.

$$\log t = A + \frac{B}{T} + \frac{C \log \sigma}{T} \quad \text{Eq. 2.4}$$

Where:

- t = failure time (hr)
- σ = applied stress
- T = test temperature (K)
- A, B and C = constants for specific material and test conditions

In order to utilize Eq. 2.4, the three constants must be determined for a given material and test conditions. Typically stress crack tests are performed at different elevated temperatures and applied stresses and the data are used to establish the three constants. A new Eq. 2.4 with known A, B and C values can then be applied to determine failure times at a specific temperature and applied stress.

3.3.4 Comparing PSM and RPM in Predicting Long-term SCR

The three sets of ductile-to-brittle curves in Figs. 2.9 and 2.10 are used to investigate the reliability of PSM and/or RPM. The verification was performed by using data at 70 and 80°C to predict and verify the ductile-to-brittle curve at 60°C, which was then compared with the experimental data to evaluate the respective methods. In Figs. 2.14 and 2.15, the solid green line at 60°C was generated by RPM using A, B and C values obtained from data at 70 and 80°C in water and air, respectively (Hsuan and Zhang, 2005). The predicted curves are very similar to the actual experimental data. For PSM, the predicted curve at 60°C was created by shifting each data point at 70 and 80°C using corresponding shift factors that were calculated according to Eqs. 2.2 and 2.3. The shifted data at 60°C were then analyzed by the ISO method to determine the ductile-to-brittle curves, which are displayed as the blue lines in both figures. It is observed that PSM over predicts the failure time at 60°C by a considerable amount.

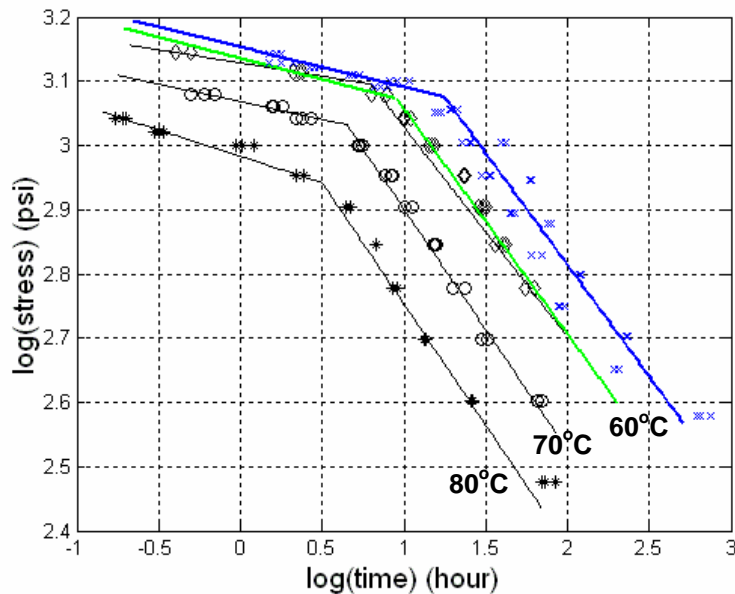


Fig. 2.14 – Experimental and predicted NCLS curves on pipe liner in water

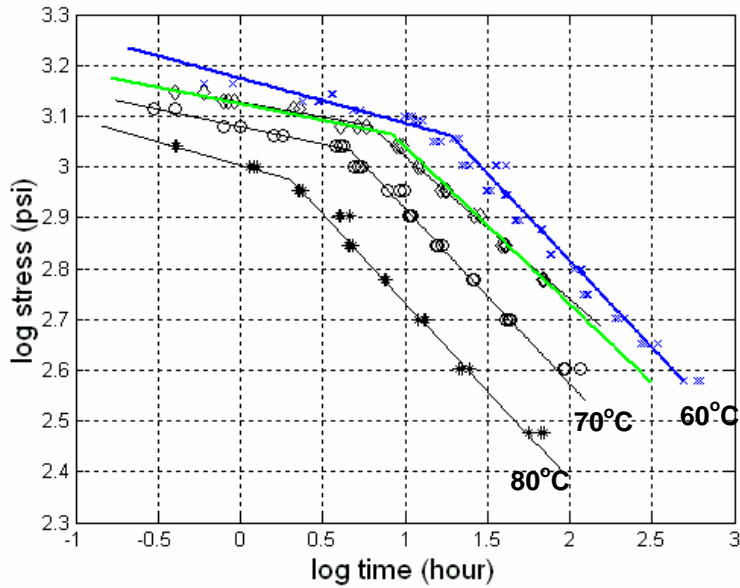


Fig. 2.15 – Experimental and predicted NCLS curves on pipe liner in air

RPM is also applied to junction test data at test temperatures of 60, 70 and 80°C from Fig. 2.13. The solid green line in Fig. 2.16 at 60°C was generated by RPM using A, B and C values obtained from data at 70 and 80°C, (recall Table 2.9). The predicted curve is fairly similar to the actual experimental data at 60°C.

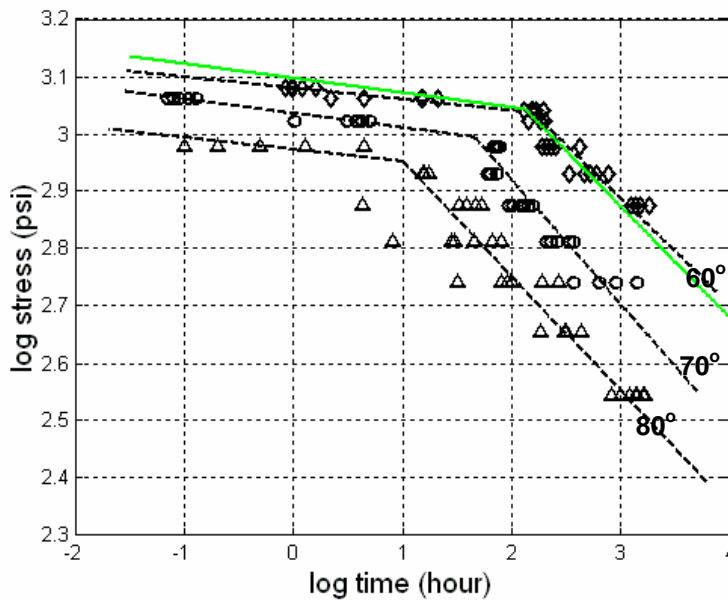


Fig. 2.16 – Experimental and predicted curves on pipe junction in water

The above analyses indicate that RPM is a more reliable method for predicting the long-term SCR of corrugated HDPE pipes. A test standard, FM 5-573, was developed to describe the prediction procedures.

In predicting a 100-year crack free pipe, junction data at 60, 70 and 80°C water were used. Fig. 2.17 shows the predicted ductile-to-brittle curve at 23°C which is identified as being the average temperature in the State of Florida. Based on the predicted curve, the failure time at 500 psi ($\log 500 = 2.7$) is well over 100 years. Recall that 500 psi is the predicted tensile stress in the pipe under long-term field conditions resulting from Part 1 of the report.

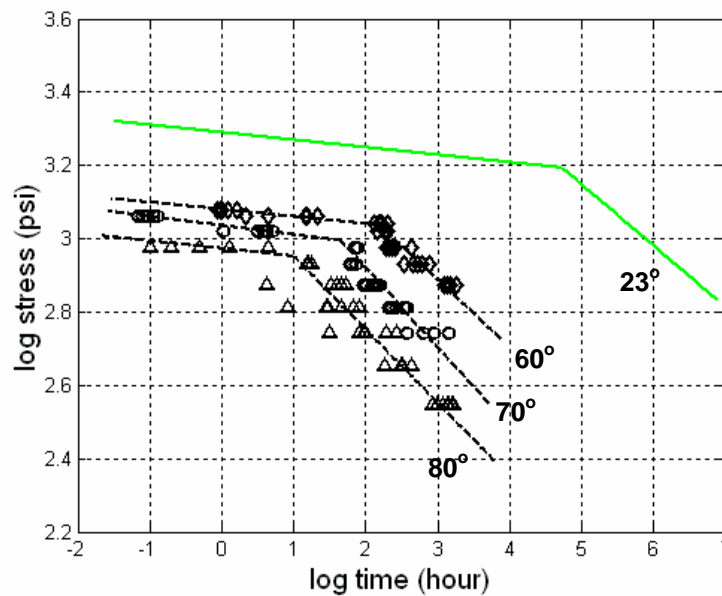


Fig. 2.17 – Predicted 23°C curve on pipe junction in water

3.4 Summary of Laboratory SCR Evaluation

The SCR of three corrugated HDPE pipes was evaluated and presented in this section of the report. The tests focused on three specific locations of the pipe which were; the inner liner, liner/corrugation junction, and longitudinal profile. A QA/QC test (FM 5-572) was developed to assess the susceptibility of the stress crack at these three locations.

In order to investigate the effect of the test media, NCLS tests were performed in three different test environments; 10% Igepal[®], water, and air. The data confirm that the 10% Igepal[®] solution provides the greatest acceleration to crack growth rate.

In predicting the long-term SCR of corrugated HDPE pipes, RPM was found to be the most appropriate of three methods evaluated. The test procedure is described in Section 5.6.1.2 of ASTM D2837, which recommends three sets of tests (two stress levels at one test temperature, and one stress level at a second temperature) to determine the three constants in Eq. 2.4. Based on the ASTM D 2837, a new test standard “FM 5-573” was developed defining the specification conditions for performing tests on corrugated pipe junctions and longitudinal profiles.

4. LABORATORY TESTS TO EVALUATE OXIDATION RESISTANCE OF CORRUGATED HDPE PIPES

4.1 Background

As shown in Table 2.1, the current AASHTO M294 specification does not require the evaluation of antioxidants in HDPE corrugated pipes except for the cell class defined in ASTM D 3350. In the NCHRP Report 429, a large variation was found in the antioxidants of 14 evaluated commercially new pipes. The data is as shown in Fig. 2.18. The amount of antioxidants in the pipe is expressed by the OIT value which ranges from few minutes to over 40 minutes. This large scatter in the data indicates that there is little consistency in the manufacture of different HDPE corrugated pipes and is a major issue of concern.

The function of antioxidants in the corrugated pipe is to protect the polyethylene resin from oxidative degradation. The mechanical properties (including SCR) can only be preserved by properly formulated antioxidants. Thus, the lifetime of antioxidants plays an essential role in the overall service life of the pipe.

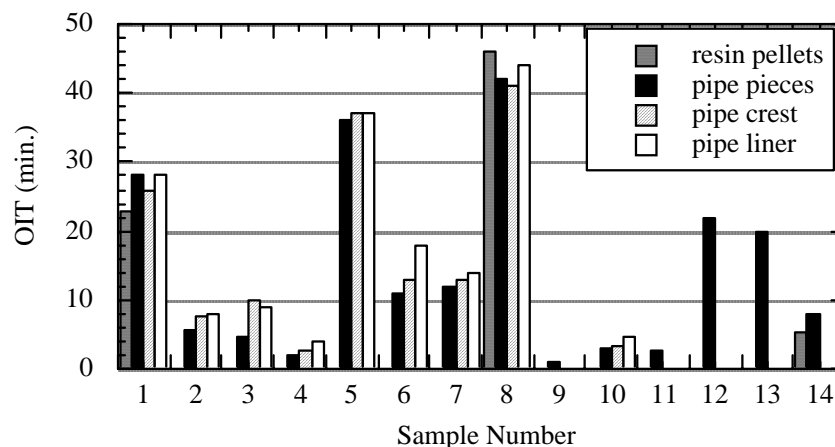
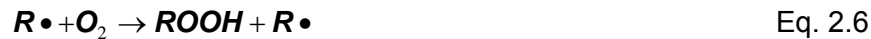


Fig. 2.18 - OIT data of fourteen commercially new pipe samples

The overall oxidation mechanisms can be divided into three conceptual stages, as shown in Fig. 2.19 (Hsuan and Koerner, 1999). These mechanisms are well established in the HDPE pressured pipe industries.

- Stage A represents time to consume all of the antioxidants in the pipe. The duration of this stage depends on both the type and amount of antioxidants as well as the site ambient environment or simulated laboratory testing conditions.
- Stage B is the induction time which is the inherent property of the unstabilized polymer. In this stage the polymer reacts with oxygen and generates free radicals and hydroperoxide (ROOH), as expressed in Eqs. 2.5 and 2.6. The duration of this stage is governed by the concentration of hydroperoxide.



- Stage C is the autocatalytic stage of the oxidation in which the formation of free radicals accelerates due to decomposition of ROOH, as indicated in Eqs. 2.7 to 2.9. The onset of the Stage C is when the hydroperoxide in the polymer increases to a critical concentration. The series of free radical reactions that take place in Stage C result in breaking polymer chains which leads to degradation in mechanical properties of the materials.



Note: In Eqs 2.5 to 2.9, *RH* represents the polymer chain and compounds with the symbol (\bullet) are free radicals.

Gedde's group has published a series of papers on the oxidation of HDPE hot water pressure pipes. Their findings are summarized in a review paper (Gedde, et al., 1994). In their study, the long-term performance of pressurized pipe was evaluated using method similar to ASTM D2837. The test pipes were subjected to a series of internal pressures using either air or water, and were incubated in both water and air environments at temperatures from 60 to 105°C. The failure modes of the pipe are illustrated in Fig. 2.20. In Stage I, pipes fail by ductile mode. In Stage II, pipes fail in brittle mode via stress crack growth. In Stage III, the effect of mechanical

loading becomes insignificant due to extremely low applied stresses, so that the pipes fail in brittle mode by oxidation degradation of the polymer. The transition between Stages II and III may sometimes be difficult to clearly define. Karlsson, et al. (1992) found that the formation of carbonyl groups which resulted from the oxidation degradation of polyethylene took place much earlier than the onset of Stage III. However, due to the low applied stress, it took a longer time for the pipe to fail than at a high applied stress.

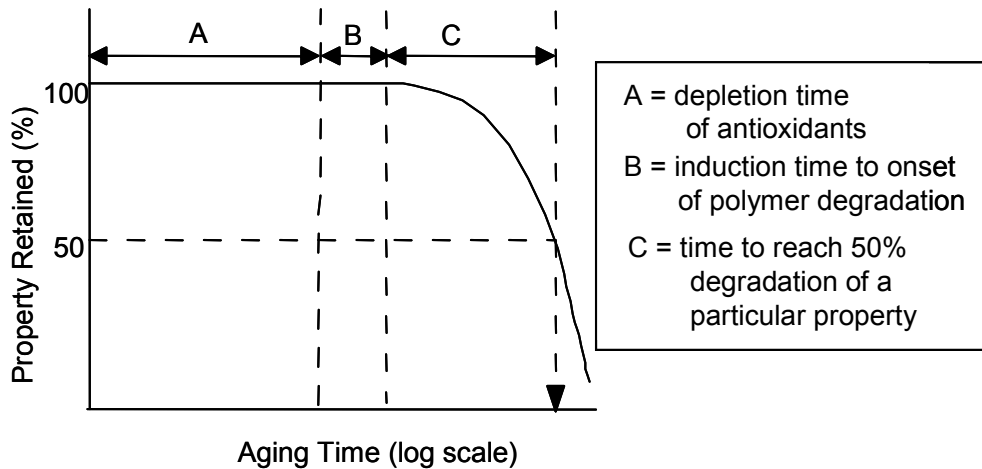


Fig. 2.19 – Three conceptual oxidation stages of HDPE

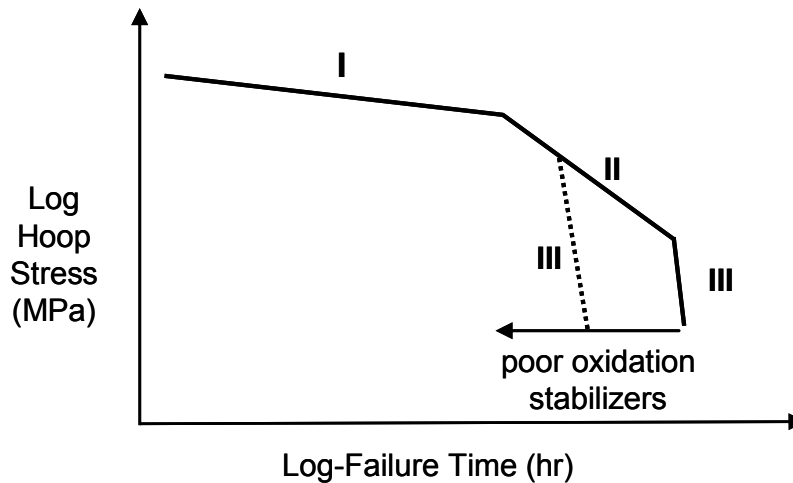


Fig. 2.20 – Three potential failure stages in pressure testing of smooth wall pipes

By comparing Figs. 2.19 and 2.20, the onset of the Stage III is within Stage C, while the exact position is dependent on the applied stress. Importantly, the onset of the Stage III must be well beyond the design life of the application under consideration. Gedde's data show that for gas

pipe with appropriate antioxidants and good stress crack resistance properties, the onset of Stage III can be predicted to 1000 years at 20°C in water and/or air environments. However, without antioxidants, the onset of Stage III shortens to 11 years (Viebke, et al, 1994). Janson (1995) extrapolated the onset of Stage III using test data that were presented by Gaube's group (Gaube, et al, 1985) and predicted 500 years at 20°C; however, the types of antioxidants in the tested pipes were not presented.

The published data on pressurized pipes clearly demonstrates the importance of the antioxidant package in the long-term performance of HDPE pipes. It is anticipated that this importance holds for corrugated drainage pipes with design life of 100-year. The complicating issue, however, is that there are many types of antioxidants from which different formulations can be generated to target performance requirements. Furthermore, each antioxidant formulation probably performs differently under air and water environments and must be evaluated accordingly. Fig. 2.21 shows the antioxidant depletion with time of five different geomembranes with unknown antioxidant formulations. The data indicate that Geomembrane E contains very different antioxidant than the other four (Hsuan and Guan, 1998).

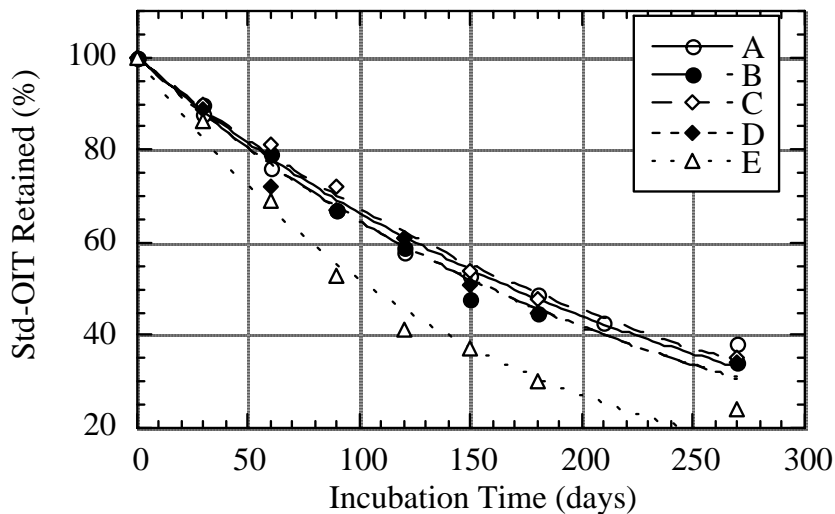


Fig. 2.21 – Depletion of antioxidants with time for five HDPE geomembranes with unknown antioxidant formulations

The pressurized pipe test is an ideal performance test that challenges the antioxidant properties and SCR simultaneously. However, it requires long testing times (on the order of years) to generate sufficient data for analysis. Alternatively, short term accelerated tests have been developed to verify the oxidation resistance of the material (Hsuan and Koerner, 1999). The

approach of the short term accelerated tests is to evaluate antioxidant performance and stress cracking separately.

4.2 Methods to Evaluate Antioxidants

For assessing antioxidant content in HDPE corrugated pipes, two tests are available. They are oxidative induction temperature (IT) and oxidation induction time (OIT). A brief description of each of the tests is presented below:

- IT – This is a dynamic test performed by heating the test specimen under air at a heat rate of 10°C/min until oxidation of polymer takes place. The test procedure is described in ASTM D 3350, but there is no separate ASTM standard written on this method. In ASTM D 3350, a 220°C IT value is specified to ensure sufficient antioxidant in the resin. However, the implication of the specified value in regard to the long-term oxidation resistance of the pipe is not stated.
- OIT – The test procedure is described in ASTM D3895. The test measures the time for the polymer to oxidize at a constant temperature of 200°C under oxygen atmosphere. The test is well-established as one of the analytical tools used to evaluate the amount of antioxidants in the polymer. The test has been used to investigate the antioxidant package in hot water pressure pipes (Karlsson, et al, 1992, Smith, et al, 1992, and Veibke and Gedde, 1998) as well as to assess and predict the lifetime of antioxidants in the HDPE geomembranes (Hsuan and Koerner (1999) and Sangam and Rowe (2002)).

The correlation between IT and OIT results was recently investigated on four different grades of polyethylene by Schmid and Affolter (2002). They found that the IT test results exhibited a significantly lower standard deviation in both repeatability and reproducibility than OIT. However, the sensitivity of the IT decreases significantly with rising temperature, as shown in Fig. 2.22. A similar finding was also observed by Karlsson, et al, 1992, as shown in Fig. 2.23. Also note that the specified IT value of 220°C in ASTM D3350 corresponds to approximately 10 minutes or less OIT based on these two graphs.

The IT test seems to be suitable for QA/QC of antioxidants in the pipe due to its low standard deviation. However, the sensitivity of the test decreases significantly when the IT value exceeds approximately 230°C. This corresponds to an OIT value between 10 and 20 minutes. Thus, for

pipes with OIT values longer than 20 minutes, the OIT test is the appropriate choice. As a result, the OIT test and its results will be used for the purposes of this study.

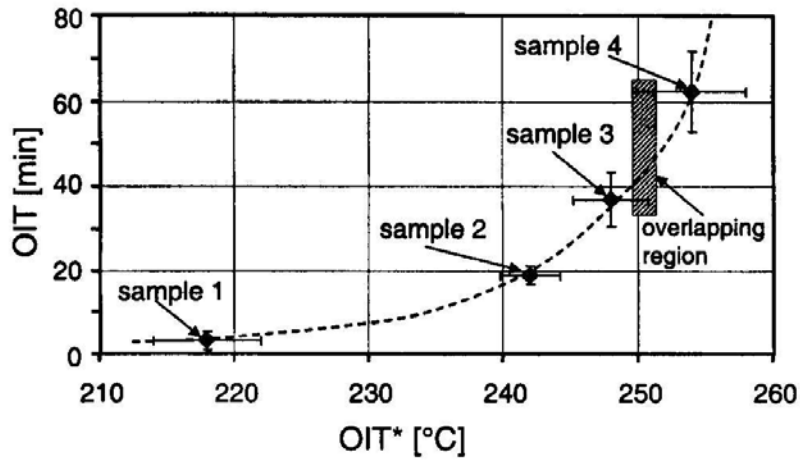


Fig. 2.22 – Correlation between OIT and IT of four polyethylene grades

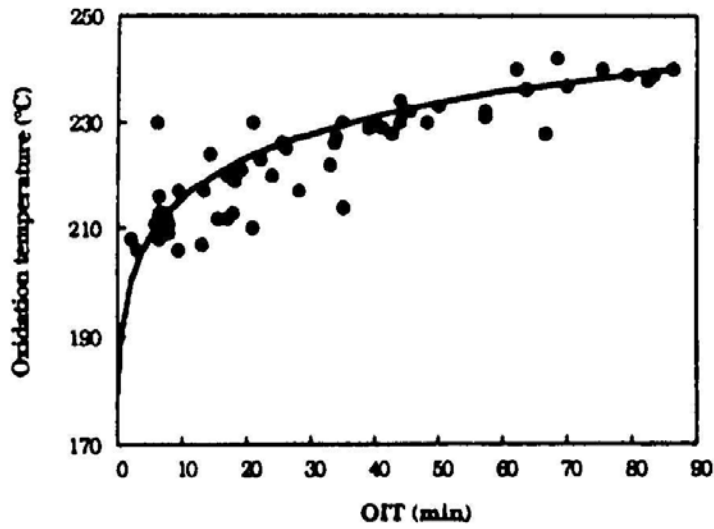


Fig. 2.23 – Correlation between IT and OIT

4.3 Accelerated Oxidation Tests

The lifetime of the antioxidants and oxidation lifetime of corrugated pipes can be predicted using accelerated tests on the basis of time-temperature superposition. An important consideration in an acceleration test is that the incubation environment should reflect the field condition of the pipe as close as possible. For corrugated drainage pipes, saturated soil should surround the outside of the pipe and circulating water should be inside the pipe. The interior of the corrugations is probably partially filled with static water. As can be suspected it is very difficult to set up a laboratory test to simulate such field conditions. It is clearly not a QA/QC test.

Complete simulation aging test is expensive and time consuming; thus, a more simplified incubation methods are developed. While the simplified methods still based on elevated temperature, their incubation is more straightforward and can be done within the constraints of this project. One is based on air incubation (in forced air ovens) and the other is water incubation (in hot water baths). Both will be described following.

4.3.1 Accelerated Oxidation in Air

Oven aging is the most widely used acceleration method to evaluate oxidation degradation of a wide variety of polymers. Test specimens are placed in a forced air oven at an elevated temperature to accelerate oxidation reactions. A minimum of three elevated temperatures should be utilized for the Arrhenius prediction method. In this laboratory test, a single elevated temperature was used for a preliminary evaluation. Samples taken from the two corrugated pipes (P-1 and P-2) were incubated in a forced air oven at 85°C. Specimens were retrieved from the crown and liner locations of the incubated pipe samples and were evaluated by the OIT test at different intervals. The resulting OIT depletion curves are shown in Figs. 2.24 and 2.25 for sample P-1 and P-2, respectively. For P-1 pipe, the antioxidant depletion rates of pipe liner and pipe crown are basically the same. Comparing the depletion rates of antioxidant in the liner part of P-1 and P-2, they are relatively similar. Some difference can be seen between these two parts in the P-2 pipe. The cause for the difference depletion rates in liner and crown of P-2 is unclear, since the thickness of these parts is relatively similar.

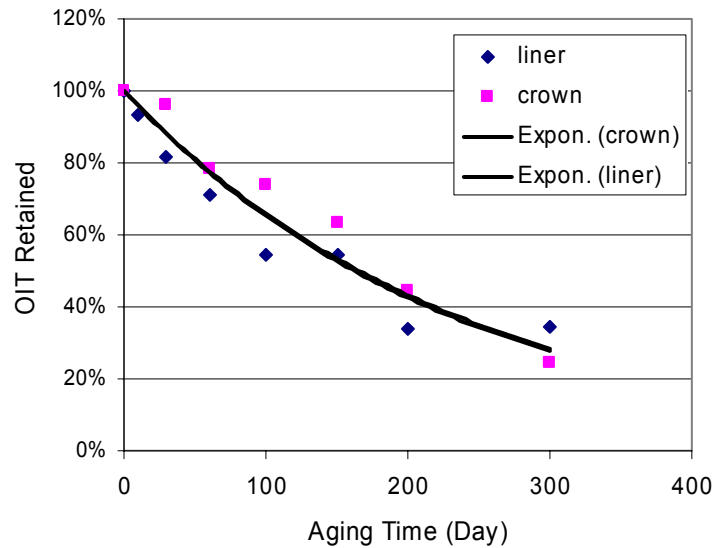


Fig. 2.24 – OIT depletion curve of P-1 in a forced air oven at 85°C

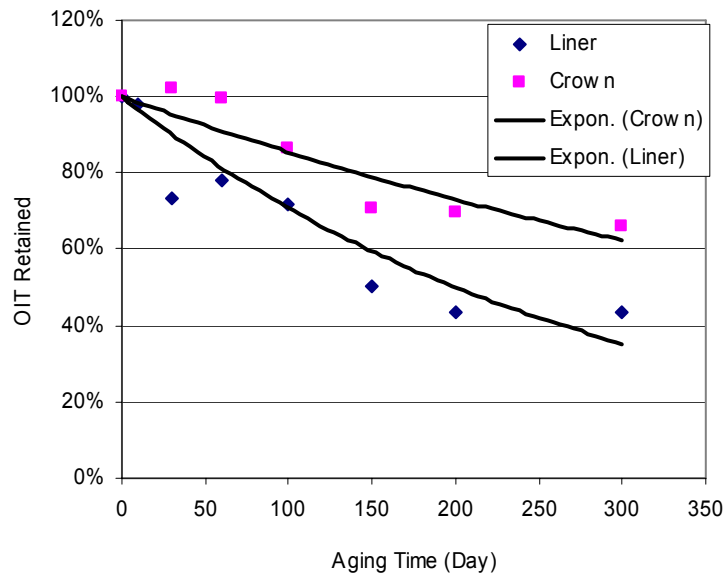


Fig. 2.25 – OIT depletion curve of P-2 in a forced air oven at 85°C

4.3.2 Accelerated Oxidation in Water

Certain types of antioxidants can be extracted by the surrounding water or can react with water in a process called hydrolysis. In this acceleration method, samples taken from the two corrugated pipes (P-1 and P-2) were incubated in a water bath at 85°C. Specimens were retrieved from the crown and liner locations of the incubated pipe samples and were evaluated by the OIT test at different intervals. The resulting OIT data are shown in Figs. 2.26 and 2.27

for Samples P-1 and P-2, respectively. On the same graph, the OIT depletion curves in air are superimposed to observe the effect of incubation environment. Here it is seen that the antioxidant depletion rates are significantly faster in water than in air, confirming the interactions between water and the antioxidants in these two pipes. Similar results were also observed in gas pipes. For example, Smith, et al. (1992) found that the antioxidant depletion rate is three time faster in water than in air.

After 90 days, however, the antioxidant depletion rates in water become almost constant and the OIT retained values maintain at 10 to 20%, entering the induction stage (Stage B) of the oxidation process. During the induction stage, the material properties remain essentially constant. Figs. 2.28 and 2.29 show the tensile properties (break strength and break elongation) and melt index (which is qualitatively related to the molecular weight) throughout 300 days of incubation, and the properties remain largely unchanged. The long induction stage in the water environment results from the low oxygen content which is less than 8% in water compared to to 20% in air; subsequently, the oxidation rate decreases significantly.

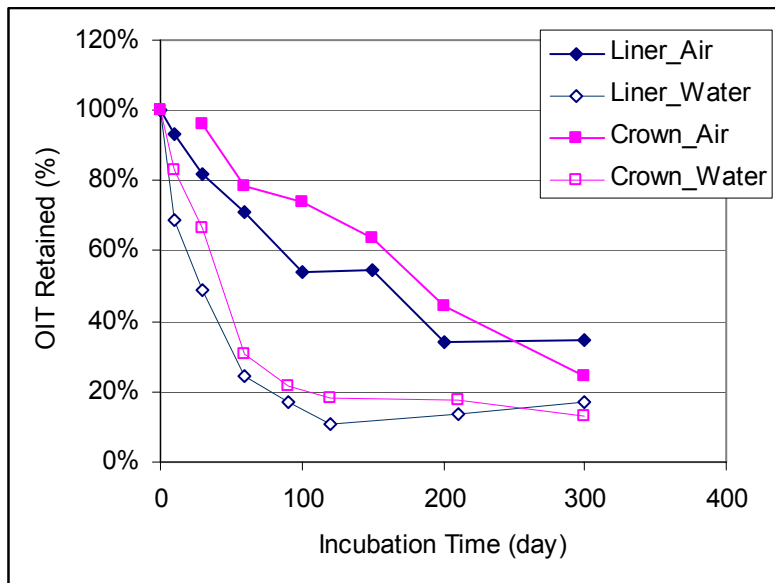


Fig. 2.26 – OIT depletion curves in air and water at 85°C of P-1

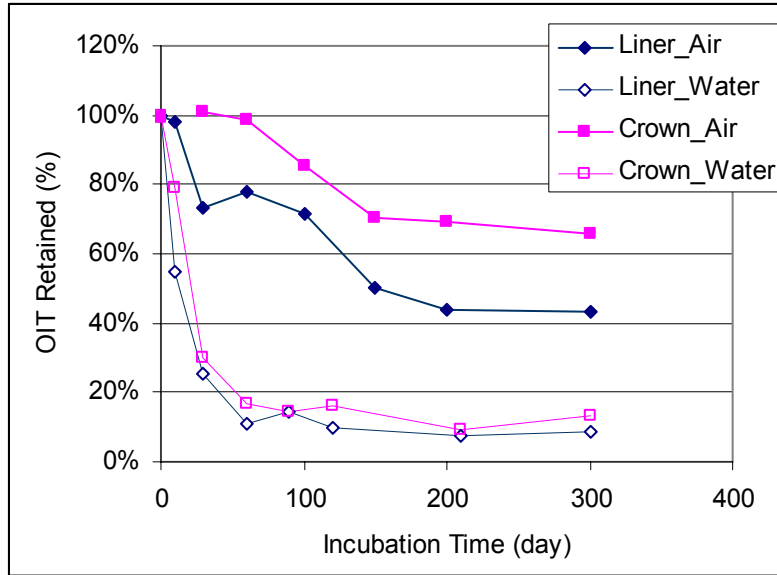


Fig. 2.27 – OIT depletion curves in air and water at 85°C of P-2

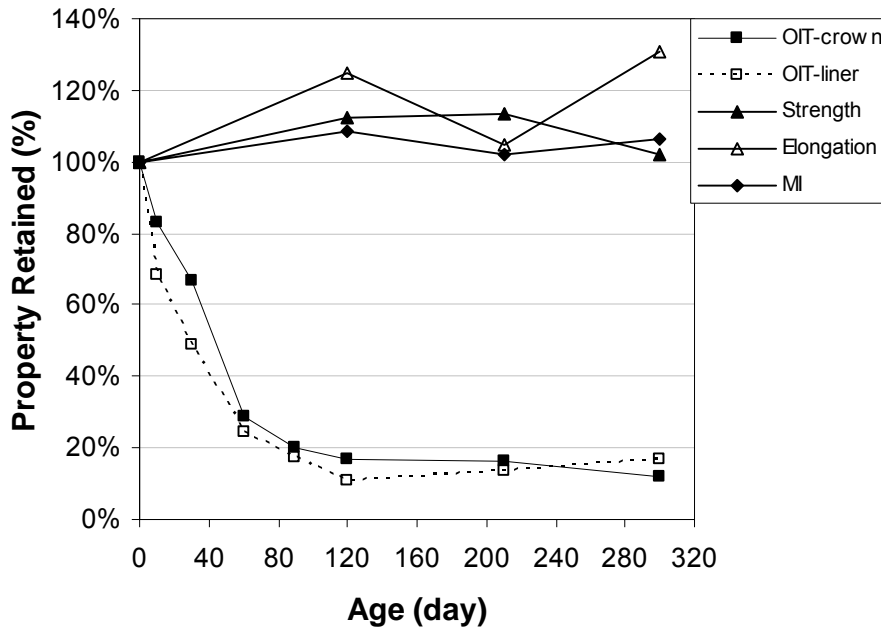


Fig. 2.28 – Material properties of P-1 versus incubation time in water at 85°C

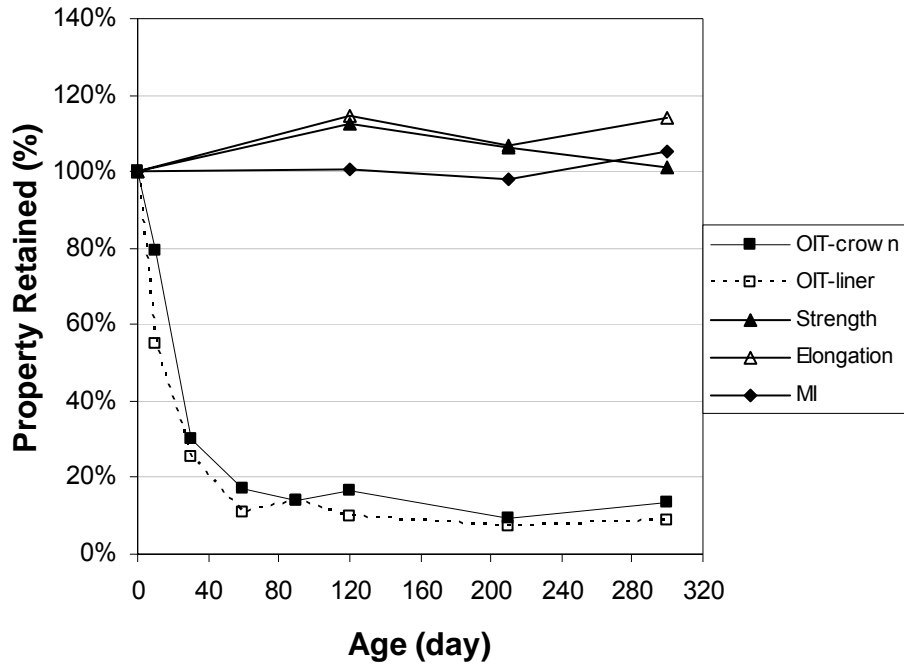


Fig. 2.29 – Material properties of P-2 versus incubation time in water at 85°C

The oxidation process in water and air environments can be schematically shown in Fig. 2.30. The duration of Stage A is expected to be longer in air than in water. On the other hand, Stages B and C would be significantly longer in water than in air, due to the limited available oxygen content in the water.

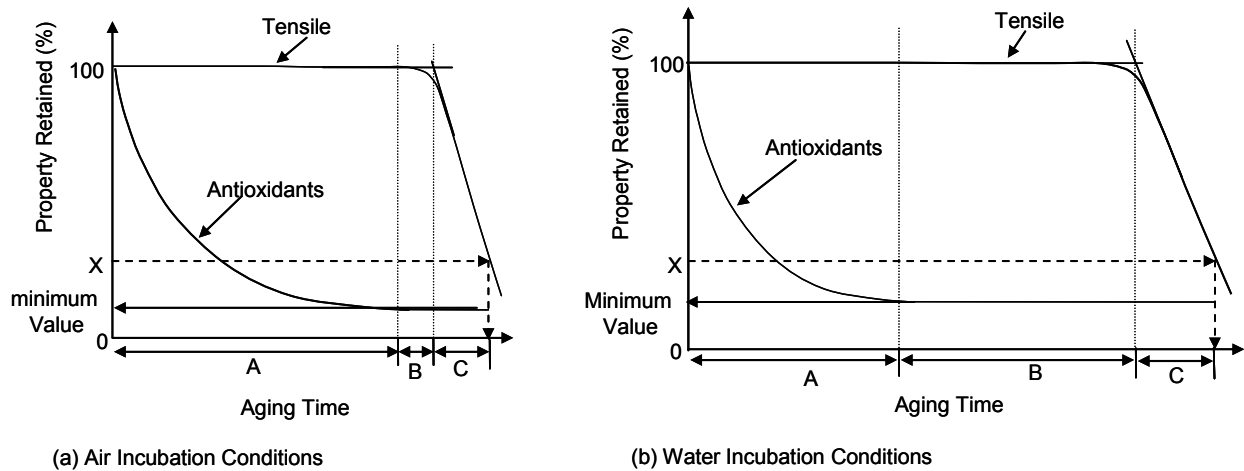


Fig. 2.30 – Three conceptual degradation stages in air and water incubation

For OIT testing in the previous sections of the report, the specimens were taken across the thickness of the incubated samples. The resulting OIT value represents the average amount of antioxidants remaining in the specimen. Concern has been raised regarding the oxidation status on the surface of the specimen. The Fourier Transform Infrared (FTIR couple with Attenuation Total Reflection device using a Germanium crystal) was used to analyze the specimen's surface. Sample P-1 after incubation in 85°C water for 2341 hours was analyzed at three locations: at the surface, 0.5 mm and 1 mm from the surface of a 2.5 mm thick specimen. The resulting FTIR spectra are shown in Fig. 2.31 together with the spectrum obtained from the original non-incubated sample. The peak at 1730 cm^{-1} would be expected from the carbonyl functional group in oxidized HDPE materials. As seen on the graphs, no peaks at this wavenumber was seen in any of the locations. Thus, this issue of surface degradation does not appear to be a concern. The broad peak around 1000 cm^{-1} is resulted from the oligomers of polyethylene (PE). It is believed that the very low molecular weight polymer diffused to surface during the high temperature incubation.

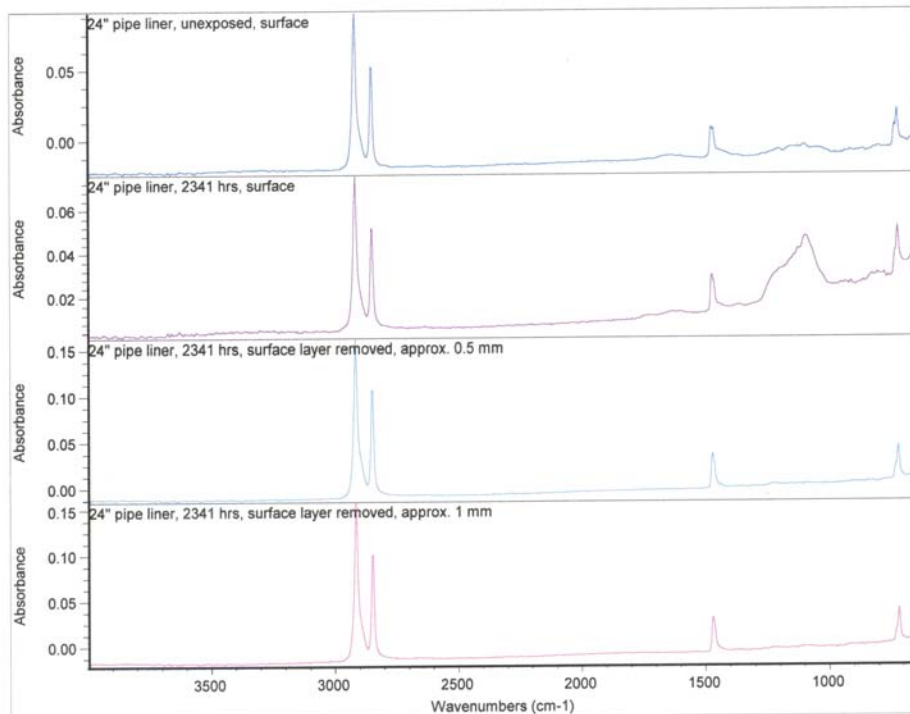


Fig. 2.31 – FTIR spectra of sample P-1 after incubation in 85°C water for 2341 hours

4.4 Determining the Initial Oxidative Induction Time Value

The determination of the minimum amount of antioxidants in the corrugated HDPE pipes should not be solely based on data from the water incubation environment performed in this study, because the outer surface of the pipe is surrounded by saturated or partially saturated soil. The assessment should consider both water and soil environments. However, there is no such data available for corrugated HDPE pipes. There is, however, considerable data for incubation in soil HDPE geomembranes (Hsuan and Koerner, 1998). Samples of a HDPE geomembrane were incubated in a specially designed chamber exposing to saturated soil above and dry soil beneath the sample under a compressive stress of 260 kPa at temperatures of 55, 65, 75, and 85°C. Incubated samples were retrieved from the chamber over time and their properties were evaluated. Also samples from the same HDPE geomembrane were incubated in water baths at the same four temperatures. The OIT value of the incubated samples was monitored with time and their relationship is expressed by Eq. 2.10 in both soil and water incubation environments.

$$\text{OIT} = P \cdot \exp(-S \cdot t) \quad \text{Eq. 2.10}$$

where:

- OIT = OIT time (min)
- P = original OIT of the geomembrane (min.)
- S = OIT depletion rate (min/day)
- t = incubation time (days)

The depletion rate can be determined from the slope of the line by plotting $\ln(\text{OIT})$ versus incubation time for each incubation temperature. By then applying the Arrhenius Equation, Eq. 2.11, the antioxidant depletion rate at site specific temperature, such as 23°C, can be predicted. As shown by Hsuan and Koerner (1998), the predicted antioxidant lifetimes (time to reach 0.5 minutes of OIT) for these HDPE geomembranes are 200 and 55 years for soil and water incubations, respectively.

$$S = A \cdot \exp(-E/RT) \quad \text{Eq. 2.11}$$

where:

- S = OIT depletion rate
- E = Activation energy of the antioxidant depletion reaction (kJ/mol)
- R = gas constant (8.31 J/mol.K)
- T = test temperature in absolute Kelvin (degrees K)
- A = constant

The two predicted lifetimes are then used to estimate the required OIT value necessary for 100 years lifetime. Fig. 2.32 shows the \ln OIT versus predicted lifetime plot for water and soil incubations. The soil/water line was generated by taking the average of the two, i.e., 127 years. The created soil/water line was then shifted to 100 years lifetime, and the corresponding OIT at zero years is 25 minutes. Thus, the minimum required OIT value in the same HDPE geomembrane to ensure 100 years antioxidant lifetime is 25 minutes. However, it should be emphasized that this is a rather conservative approach. As illustrated in Fig. 2.29, the properties do not decrease immediately after the depletion of antioxidant. The lifetime (typically defined at 50% change in tensile properties) would be much longer than 100 years, depending on the site conditions.

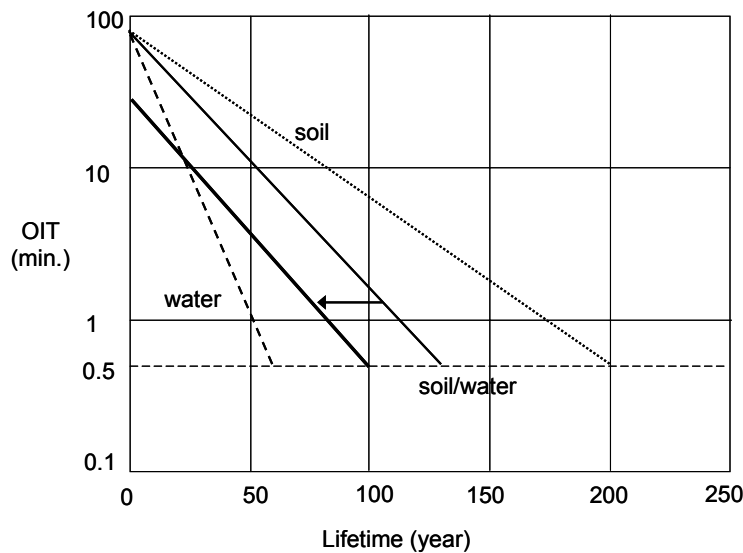


Fig. 2.32 – Plot \ln (OIT) versus predicted lifetime

4.5 Assessing Oxidation Resistance

It is important to recognize that the OIT value of unaged pipes do not totally reflect the performance of antioxidants, since certain antioxidants can produce a high OIT value at the test temperature of 200°C. In order to properly assess the antioxidant package, the depletion rate of antioxidants should also be determined by measuring the OIT value after a given incubation duration (the slope of the line in Fig. 2.31).

The incubation duration is based on 100-year lifetime of antioxidants at site temperature of 23°C. A corrugated HDPE pipe sample was immersed in a water bath at a temperature of 80°C.

The duration of the incubated was obtained based on the Arrhenius equation and is 187 days, as shown in the following calculation, Eq. 2.12. An activation energy of 75 kJ/mol for the unstabilized polyethylene was used as a conservative approach. (Note that the activation energy of stabilized HDPE is 110 kJ/mol.)

$$\frac{876000hr}{t} = \exp\left[\frac{-E}{R}\left(\frac{1}{80 + 273K} - \frac{1}{23 + 273K}\right)\right]$$

$$\frac{876000hr}{t} = \exp\left[\frac{-75000J/mol}{8.341J/mol - K}\left(\frac{1}{80 + 273K} - \frac{1}{23 + 273K}\right)\right] \quad \text{Eq. 2.12}$$

$$t = 6346hr \text{ (264days)}$$

Furthermore, a constant tensile stress of 250 psi is applied to the specimen during incubation to reflect the long-term tensile stress in the pipe under field conditions. The OIT retained value after 264 days of incubation should be 3-minute which is the value resulting from Samples P-1 and P-2.

4.6 Summary of Laboratory Oxidation Resistance Evaluation

This preliminary study on oxidation resistance of two HDPE corrugated pipes was evaluated via the depletion of antioxidants under water and air environments. The results indicate that the depletion of antioxidants is significantly faster in water than in air. However, the onset of oxidation is suppressed due to the limited oxygen content in the water.

The initial OIT value of 25 minutes in the corrugated HDPE pipe samples was determined using data from HDPE geomembranes under a soil/water environment. The antioxidant depletion rate was assessed in a water environment at 85°C under 250 psi tensile stress. After 187 days of incubation, the OIT retained should be 3-minutes.

A Florida Method of Test FM 5-574 was developed to describe the laboratory evaluation on the oxidation resistance of corrugated HDPE pipe, including the determination of depletion rate of antioxidants, lifetime of antioxidants, and oxidation lifetime of the pipe.

5. LABORATORY TESTS TO EVALUATE LONG TERM DESIGN PARAMETERS OF HDPE CORRUGATED PIPES

5.1 Background

The current design parameters for corrugated HDPE pipe specified by AASHTO Section 17 is shown in Table 2.10.

Table 2.10 – Mechanical Properties for Design Corrugated HDPE Pipes

Short Term Properties		50-year Long Term Properties	
Tensile Strength	Modulus of Elasticity	Tensile Strength	Modulus of Elasticity
3,000 psi	110,000 psi	900 psi	22,000 psi

The short term tensile strength and modulus of elasticity are taken from the material specification ASTM D3350 based on a cell class of 335400C. Using compressive molded plaques (and not the finished pipe), the extrusion processing effects are not present. A part of this section of the laboratory tests is to investigate the possible differences in mechanical properties between compressive molded plaques and the as-manufactured pipe materials.

For the long term property values, AASHTO Section 17 states that “these values are derived from hydrostatic design bases (HDB) and indicate a minimum 50-year life expectancy under continuous application of tensile stress”. Thus, the values listed in Table 2.10 were obtained under a creep mode. Since HDB testing was removed from the AASHTO Section 18 Bridge specification after 1996, the verification of the long term properties is questionable. Furthermore, the HDB test is not the appropriate test to evaluate corrugated pipes, since corrugated pipes are not subjected to constant internal pressure during service.

In this portion of the project, an alternative creep test is presented to determine the long-term tensile strength of pipe. In addition, the long-term modulus value is evaluated based on stress relaxation mode instead of creep mode to reflect the in-situ condition of the pipe.

5.2 Tensile Properties of Pipes

The short term tensile strength listed in Table 2.10 is obtained from test specimens taken from compression molded plaques of pure resins; hence, the effects of the pipe manufacturing

process and carbon black additives on the tensile properties are not considered. For the evaluation the tensile properties of the finished pipe, the liner part of the pipe is utilized for the test. ASTM D638 was used to test the pipe liner. Depending on the width of the liner between two junctions, either Type VI or V die was used. Table 2.11 shows the appropriate types of dies to be used to evaluate tensile properties of the pipe liner. The tensile specimens shall be oriented along the longitudinal axis of the pipe. Both Types IV and V tests shall be performed at a strain rate of 2 inch/min. The gauge lengths are 2.5 inches and 0.3 inch for Type IV and Type V tests, respectively.

Table 2.11 – Type of Die used in ASTM D 638 for Different Pipe Diameters

Pipe Diameter (inch)	Type of Die used in ASTM D 638
18 to 42	Type V
48 to 60	Type IV

A comparison of tensile properties between molded plaque and pipe liner was carried out on pipes P-1 and P-2. Table 2.12 shows the average tensile strength value of the tests. The data in Table 2.12 indicate that the tensile strength of Type V die is slightly higher than that of Type IV. The factor is approximately 1.04. In addition, the tensile strength of the pipe liner is slightly lower than that of the corresponding molded plaque based on Type V tensile tests. The difference between these materials is not the same for pipes P-1 and P-2. This suggests that the tensile strength is affected by the pipe manufacturing process, but not significantly.

Table 2.12 – Average Tensile Yield Strength from Molded Plaque and Pipe Liner

Test Material	Type IV	Type V
P-1 (plaque)	4043	4155
P-1 (liner)		3625
P-2 (plaque)	3688	3867
P-2 (liner)		3578

5.3 Long-term Tensile Strength

As stated in Section 5.1, the 50-year long-term tensile strength of 900 psi was obtained using the HDB test (ASTM D 2837). The test provides the procedure to extrapolate test data to 50 years. However, the HDB test does not reflect the service performance of corrugated pipe, and

the test cannot be performed on corrugated pipes. Therefore, an alternative method must be employed to assess the long term tensile strength of corrugated pipe.

A new test, Florida Test Method FM 5-575 entitled, "Creep Rupture of Corrugated Pipe Liner Tensile Specimens", basically follows the concepts of ASTM D 2018. The appropriate type of tensile specimens (see Table 2.11) shall be removed from the liner part of the corrugated pipe in the orientation parallel to the longitudinal axis of the pipe. The un-notched tensile specimens are subjected to a range of applied stresses in order to establish the stress-failure time curve in a water or air environment. Elevated temperatures from 50 to 80°C can be used to accelerate the creep mechanisms.

Fig. 2.33 and 2.34 are published data on hydrostatic burst test results of HDPE smooth pipes (Popelar et al., 1991). The burst tests were performed at four different temperatures and their stress versus failure time were plotted in a log-log scale, as shown in Fig. 2.33. By applying the appropriate shift factors, the elevated failure points were shifted to 20°C, as shown in Fig. 2.34. The resulting master curve at 20°C consisted of data extending to 100 years. The same methodology can be applied to corrugated pipe using the tensile creep data. The prediction procedures are described in the Florida Test Method FM 5-576 entitled, "Determining the Long-term Tensile Strength of HDPE Corrugated Pipe".

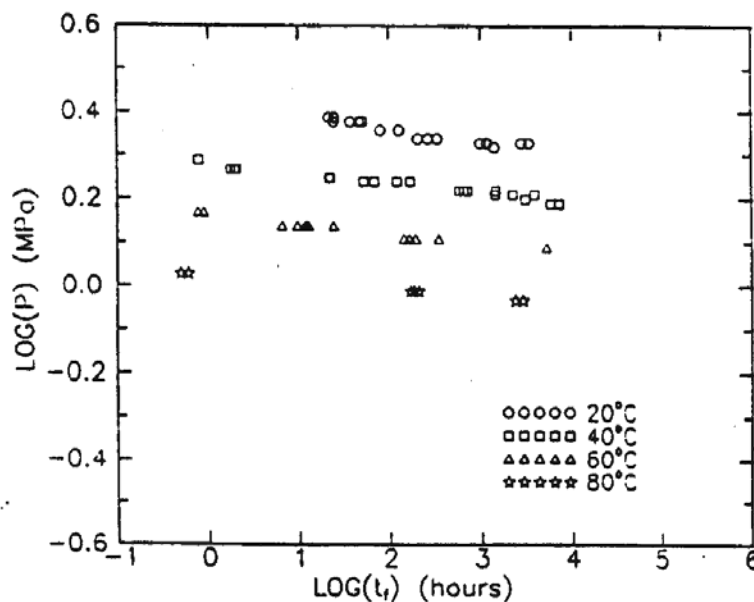


Fig. 2.33 – Hydrostatic burst pressure test data on smooth HDPE pipes

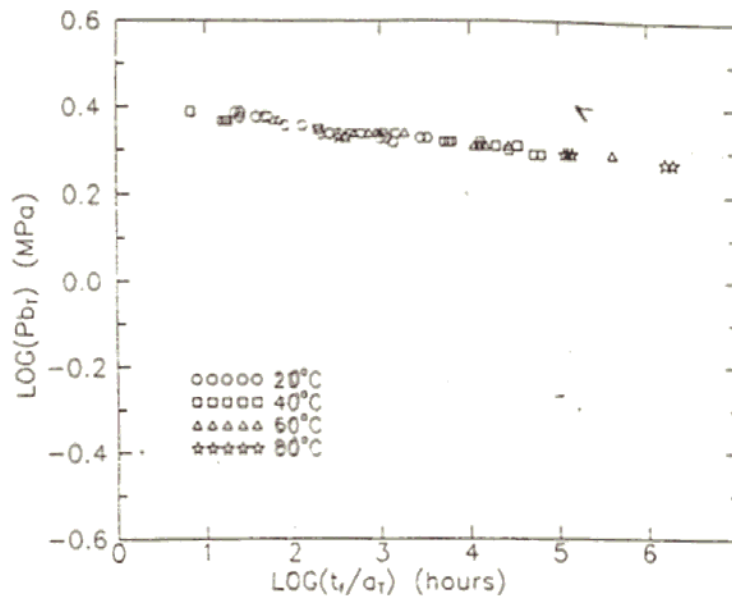


Fig. 2.34 – Obtaining master curve by shifted data in Fig. 2.33 to 20°C

5.4 Flexural Modulus of Pipes

The flexural modulus listed in Table 2.10 represents the 2% secant modulus of a 3-point bending test according to ASTM 790, Method 1-Procedure B. The test material is obtained by compression molded resin material and not the finished pipe. However, the 3-point bending test is not suitable to evaluate pipe liner of different size diameters. For small diameter pipes (less than 24 inches), the length of the liner between corrugations is too short for a 3-in long bending specimen. In addition, the liner thickness for small diameter pipes is too thin to be tested using the 2 in. span distance as defined in the ASTM 790.

For finished pipes, the method to evaluate the flexural modulus is ASTM 2412. In Appendix X2 of the standard method, the relationship between pipe stiffness and flexural modulus at a given deflection is expressed as Eq. 2.13.

$$EI = (SF) = 0.149r^3 (PS) \quad \text{Eq. 2.13}$$

Where:

$$E = \text{flexural modulus (lb/in}^2\text{)}$$

I = moment of Inertia = $t^3/12$ (in³)
 t = wall thickness of the pipe (in)
 r = radius of the pipe (in)
PS = pipe stiffness = $F/\Delta y$ (as determined by test) (lb/in/in)
 F = load per liner inch (lb/in)
 Δy = vertical deflection (in)

A comparison was made on the difference between 2% secant modulus and flexural modulus at 2% vertical deflection using pipe P-2. A force versus deflection curve of P-2 was provided by the pipe manufacturer. The inner diameter of the pipe is 24 in. and the length of the test pipe is 27 inches. To achieve 2% vertical deflection, Δy shall be 0.48 in. Using Eq. 2.13, the calculated flexural modulus value for P-2 is 109,000 psi, whereas 2% secant modulus of the P-2 pipe plaque was measured to be 118,000 psi. These two flexural modulus values are relatively similar considering that they are obtained from two very different tests.

5.5 Long-term Flexural Modulus

For the evaluation of flexural modulus of finished pipes, the parallel plate test (ASTM D 2412) is the only standard available. The test should be carried out at a deflection of 5%, which is the maximum allowable deflection value under a stress relaxation mode to reflect the condition of the pipe in the field throughout its service life. However, the test would be impractical for large diameter pipes, particularly so when testing utilizes a series of elevated temperatures. An alternative test to assess flexural modulus of finished pipes should be investigated. Gabriel and Goddard (1999) developed a curved beam test using a half pipe specimen to simulate the parallel plate test. They also performed stress relaxation tests on seven different half pipes using the curved beam test. However, the tests were carried out at room temperature, making a 100-year exploration questionable.

Due to the short duration of the project, long term stress relaxation tests based on ASTM D 2412 were not performed. On the other hand, stress relaxation tests were performed using a Dynamic Mechanical Analyzer (DMA) to illustrate the concept of Time-Temperature Superposition (T-T-S) from which a master curve at the site temperature can be obtained.

DMA tests were performed using pipe liner material from pipe P-2. The specimen was clamped between two mechanical arms, as shown in Fig. 2.35. Bending was introduced to the test

specimen. The deformation of the test specimen is illustrated in Fig. 2.36. The “X” is the bending deformation which was 0.04%.

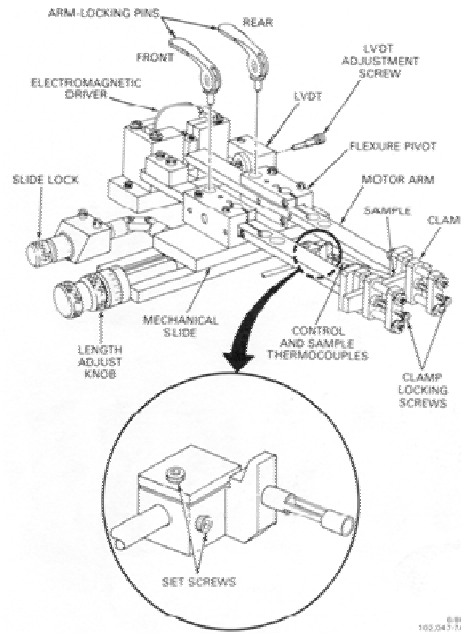


Figure 1.6
DMA Internal Components

Fig. 2.35 – Configuration of specimen clamping system in DMA

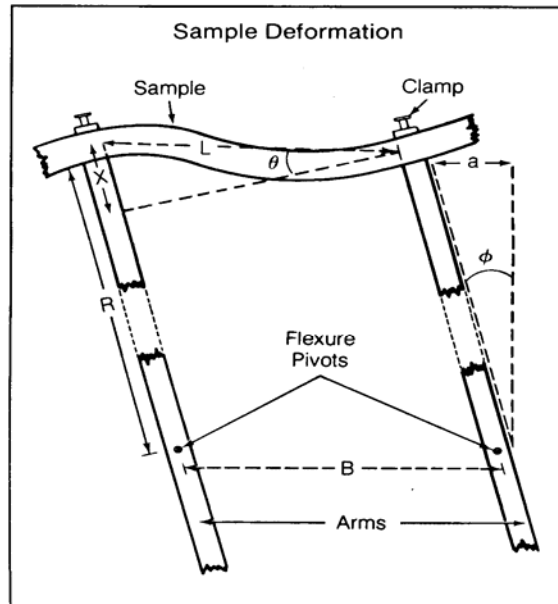


Figure 4.6
Sample Deformation

Fig. 2.36 – Deformation of the test specimen in DMA

The stress relaxation tests were carried out at temperatures from 27.5 to 65°C at 7.5°C increments. The duration of each test was 10 hours. Fig. 2.37 shows the stress relaxation curve at each temperature. The six curves were then shifted using the T-T-S software provided by the DMA manufacturer (TA Instruments). The resulting master curve at 27.5°C is shown in Fig. 2.38. In this set of tests, the master curve was extended to 1.4 years. The same set of data was also shifted using Popelar factors and the shifted data are shown in Fig. 2.39. The master curve only extended to 1000 hours, which is much shorter than the T-T-S method.

In the second set of tests, the duration of each stress relaxation test was increased to 16.7 hours. The resulting master curve at 27.5°C is extended to 13 years, as shown in Fig. 2.40. The long-term relaxation modulus values were 16% and 17.6% at 1.4 and 13 years, respectively. Table 2.13 shows the short term and long term modulus values. By extrapolating the curve in Fig. 2.40 to 100 years, the long-term modulus value is approximately 17,000 psi.

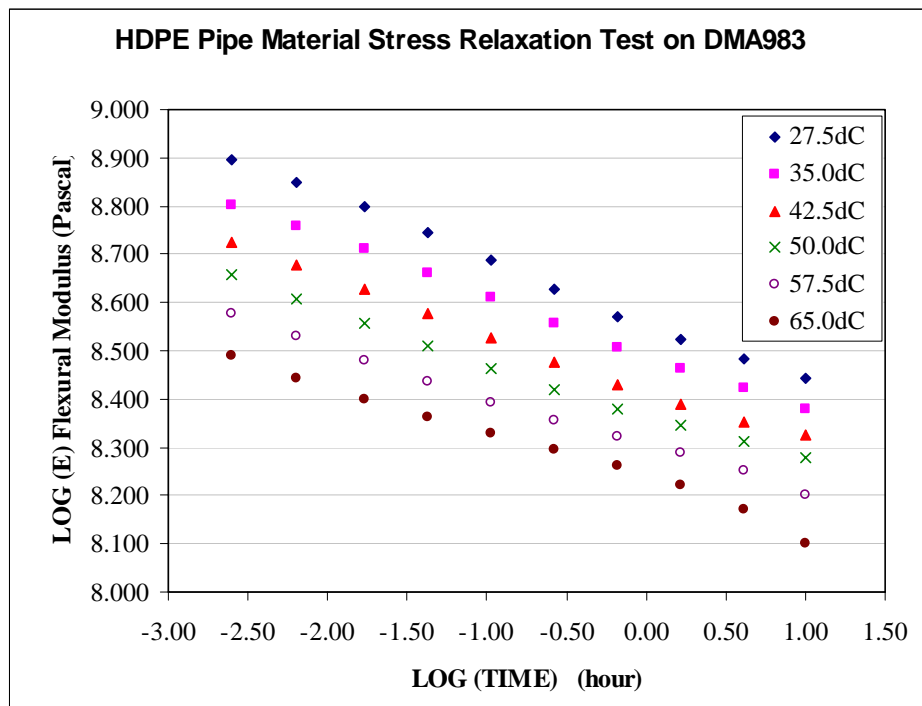


Fig. 2.37 – Stress relaxation curves resulted from the DMA test-1

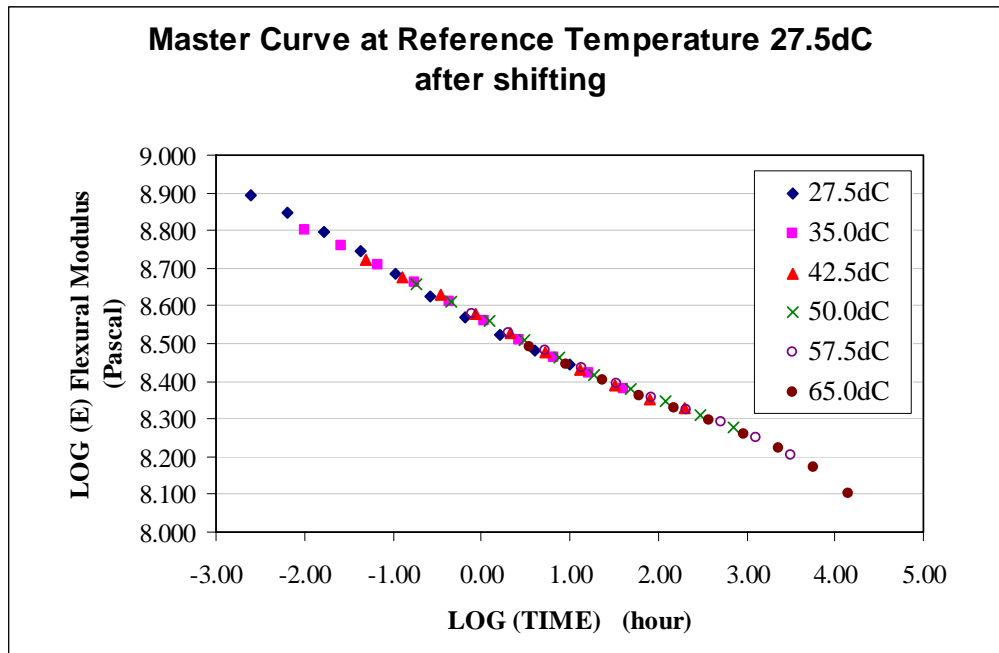


Fig. 2.38 – Master curve at 27.5°C after shifting using the T-T-S software

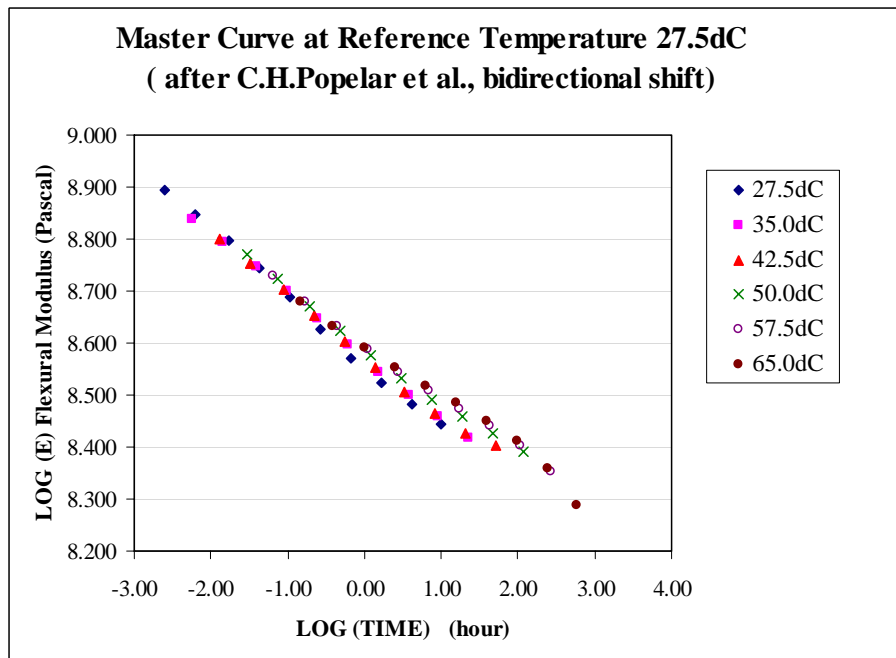


Fig. 2.39 - Master curve at 27.5°C after shifting using Popelar factors

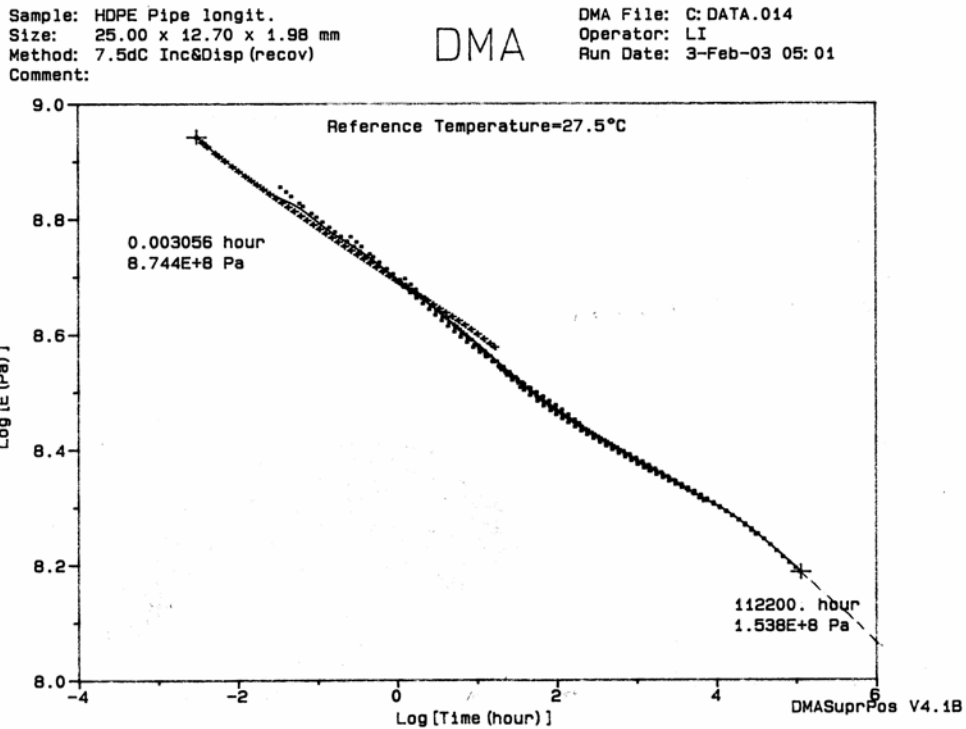


Fig. 2.40 – Master Curve at 27.5°C from DMA test-2

Table 2.13 – Flexural Modulus obtained from DMA tests

Test-1		Test-2		
Initial	1.4 years	Initial	13 years	100 years (extrapolated)
113,800 psi	18,250 psi	126,700 psi	22,300 psi	17,000 psi

5.6 Summary of Long-Term Mechanical Properties

The currently specified 50-year properties of HDPE pressured pipes were evaluated based on the HDB method, which is not suitable for use on corrugated HDPE pipes. In addition, short term properties were according to the resin cell class defined in the ASTM D 3350, not on the finished pipes. Laboratory tests were performed to assess the tensile strength and 2% flexural modulus between compression molded pipe plaque and finished pipe. The differences are relatively small. However, values from the finish pipe are approximately 10% lower than the corresponding molded plaque material.

For long-term properties, tests should be performed using finished pipes. Two new test methods (FM 5-575 and FM 5-576) were developed to assess long-term tensile strength of corrugated pipe liner material. For the long-term flexural modulus value of the pipe, the parallel plate test (ASTM D 2412) is the only standard test and should be used. The test should be performed under a stress relaxation condition at 5% deflection, at a series of elevated temperatures, as described in FM 5-577. At this time, the test is limited to pipes 24 inch diameter and less for practical purpose.

For 100-year properties, both tensile and flexural tests should utilize elevated temperatures to accelerate the viscoelastic properties and then extrapolate to the site temperature of 23°C using either the T-T-S or Popelar shift factors. The DMA results suggest that Popelar shift factors predict a shorter time than the T-T-S due to bi-axial shift.

6. SPECIFICATION

A specification for HDPE corrugated pipes to assure 100-year performance is summarized in this section. The specification consists of two parts: an interim specification and a full specification. The details of the interim specification are presented in Table 2.14. The interim specification focuses on two major properties: stress crack resistance and antioxidant content and depletion rate. In the interim specification, each required test is based on go-or-no-go criterion under specific test conditions. The specified values are determined using published data from other HDPE products.

In the full specification, four properties, stress crack resistance, oxidation degradation, long-term tensile strength, and long-term flexural modulus are required. The details of the full specification are presented in Table 2.15. For each property, a set of tests at different temperatures and/or stresses shall be performed so that the 100-year behavior of the pipe at a site temperature of 23°C can be extrapolated and determined with confidence.

Table 2.14 – Interim Specification for Long-Term Performance of Corrugated HDPE Pipes

<i>Stress Crack Resistance of Pipes</i>			
Pipe Location	Test Method	Test Conditions	Requirement
Pipe Liner	FM 5-572, Procedure A	10% Igepal solution at 50°C; 600 psi applied stress with 5 replicates	Average failure time of the pipe liner shall be ≥ 17 hours; no single value shall be less than 12 hours.
Pipe Corrugation* (molded plaque)	ASTM F 2136	10% Igepal solution at 50°C; 600 psi applied stress	Average failure time shall be ≥24 hours; no single value shall be less than 17 hours.
Junction**	FM 5-572, Procedure B and FM 5-573 ASTM D 2837	Test temperature 80°C and applied stresses of 650 and 450 psi. Test temperature 70°C and applied stress of 650 psi; 5 replicates at each stress level	Calculate three constants Failure time at 500 psi at 23°C ≥ 100 years (95% statistical confidence)
		Single Test: Test temperature 80°C and applied stress of 650 psi. 5 replicates	The failure time must be equal or greater than the calculated value using the three constants from the three point test
Longitudinal Profile**	FM 5-572, Procedure C, and FM 5-573 ASTM D 2837	Test temperature 80°C and applied stresses of 650 and 450 psi; Test temperature 70°C at applied stress of 650 psi; 5 replicates at each stress level	Calculate three constants Failure time at 500 psi at 23°C ≥ 100 years (95% statistical confidence)
		Single Test: Test temperature 80°C and applied stress of 650 psi; 5 replicates	The failure time must be equal or greater than the calculated value using the three constants from the three points test
<i>Oxidation Resistance of Pipes</i>			
Pipe Location	Test Method	Test Conditions	Requirement
Liner and/or Crown	OIT Test (ASTM D 3895)	2 replicates (to determine initial OIT value)	25 minutes, minimum
Liner and/or Crown	Incubation test FM 5-574 and OIT test ASTM D 3895	Three samples for incubation of 264 days at 80°C and applied stress of 250 psi. One OIT test per each sample.	Average OIT value shall be ≥ 3 minutes (no single value shall be less than 2 minutes)
<p>Note: FM= Florida Method of Test. * Required only when corrugation resin is different than liner resin. ** A higher test temperature (90°C) may be used if supporting test data acceptable to the State Materials Engineer is submitted and approved in writing.</p>			

Table 2.15 – Full Specification for Long-Term Performance of Corrugated HDPE Pipes

Pipe Location	Test Method	Test Conditions	Requirement
<i>Part I – Stress Crack Properties of Pipe</i>			
Pipe Liner	FM 5-572, Procedure A	10% Igepal solution at 50°C 600 psi applied stress; 5 replicates	Average failure time of the pipe liner shall be ≥ 17 hours; no single value shall be less than 12 hours.
Pipe Corrugation* (molded plaque)	ASTM F 2136	10% Igepal solution at 50°C 600 psi applied stress	Average failure time shall be ≥ 24 hours; no single value shall be less than 17 hours.
Junction**	FM 5-572, Procedure B and FM 5-573 ASTM D 2837	Test temperature 80°C and applied stresses of 650 and 450 psi; Test temperature 70°C and applied stress of 650 psi; 5 replicates at each stress level	Calculate three constants Failure time at 500 psi at 23°C ≥ 100 years (95% statistical confidence)
		Single Test: Test temperature 80°C and applied stress of 650 psi. 5 replicates	The failure time must be equal or greater than the calculated value using the three constants from the three points test
Longitudinal Profile**	FM 5-572, Procedure C, and FM 5-573 ASTM D 2837	Test temperature 80°C and applied stresses of 650 and 450 psi; Test temperature 70°C at applied stress of 650 psi; 5 replicates at each stress level	Calculate three constants Failure time at 500 psi at 23°C ≥ 100 years (95% statistical confidence)
		Single Test: Test temperature 80°C and applied stress of 650 psi., 5 replicates	The failure time must be equal or greater than the calculated value using the three constants from the three points test
<i>Part II – Oxidation Resistance of Pipe</i>			
Liner and/or Crown	OIT Test (ASTM D 3895)	2 replicates (to determine initial OIT value)	25 minutes, minimum
Liner and/or Crown	Incubation test FM 5-574, Procedure A, and ASTM D 3895	Three samples for incubation of 264 days at 80°C and applied stress of 250 psi; One OIT test per each sample.	Average OIT value shall be ≥ 3 minutes (no single value shall be less than 2 minutes)

Table 2.15 – Continue

Pipe Location	Test Method	Test Conditions	Requirement
<i>Part III – Long-Term Tensile Strength</i>			
Liner	FM 5-575 and FM 5-576	<ul style="list-style-type: none"> • Creep rupture test in water at 65, 75 and 85°C • Generate brittle curve at each test temperature 	<ul style="list-style-type: none"> • Shift elevated temperature data to 23°C • Determine tensile strength at 100 years
<i>Part IV – Long-Term Flexural Modulus</i>			
Pipe	FM 5-577	<ul style="list-style-type: none"> • Stress relaxation test in air from 35 to 85°C • Obtain the modulus versus time curve at each temperature 	<ul style="list-style-type: none"> • Shift elevated temperature data to 23°C • Determine modulus value at 100 years

7. CONCLUSIONS

Four long-term material properties of HDPE corrugated pipes were investigated in this project. These four properties include stress cracking resistance of the pipe, antioxidant lifetime of the pipe, long-term tensile strength, and long-term flexural modulus. Based on the results of this study, the following are the conclusions:

Stress crack resistance (SCR) of HDPE corrugated pipes

- i) SCR of the pipe liner is affected by the manufacturing processing
- ii) Pipe junctions and longitudinal profiles (such as vent-hole) are susceptible to stress cracking.
- iii) Stress crack growth mechanisms are very similar in water and 10% Igepal. The 10% Igepal solution was shown to accelerate the crack growth 1.7 times faster than water.
- iv) RPM is the most reliable method to predict SCR test data at the lower site temperature from elevated tested temperatures.

Antioxidants stability of HDPE corrugated pipes

- i) The types and amount of antioxidants are critical to the overall lifetime of corrugated HDPE pipe.

- ii) Between the OIT and IT methods, the OIT is the appropriate test to assess antioxidants with OIT values longer than 20 minutes.
- iii) Due to interactions between antioxidants and water, the depletion of antioxidants is more severe in water than in air.
- iv) The minimum OIT value of 25 minutes for unaged corrugated HDPE pipes was determined based on soil/water environment.
- v) The maximum antioxidant depletion rate is to be evaluated by incubating pipe samples under tensile stresses of 250 psi at 80°C water bath for a duration of 264 days. The OIT retained value shall be 3 minutes or longer.

Long-term tensile strength and flexural modulus

- i) The tensile strength of pipe liners are slightly lower than the corresponding molded plaques.
- ii) Creep rupture tests on pipe liner at elevated temperatures should be used to determine the long-term tensile strength.
- iii) The flexural modulus of the 3-point bend test from molded plaques and 2% modulus from parallel plate tests are relatively similar.
- iv) Parallel plate tests at 5% deformation under a stress relaxation mode should be used to determine the long-term modulus value.
- v) The master curve generated from Popelar shift factors is more conservative than that from the time-temperature superposition method.

8. REFERENCES

Gabriel, L.H. and Goddard, J.B. (1999), "Curved Beam Stiffness for Thermoplastic Gravity-Flow Drainage Pipes", Transportation Research Board, January, Washing, D.C.

Gaube, E., Gebler, H., Muller, W. and Gondro, C., (1985), "Zeitstandfestigkeit und Alterung von Rohren aus HDPE", Kunststoffe 75, pp. 412-415.

Gedde, U.W., Viebke, J., Leijstrom, H. and Ifwarson, M. (1994), "Long-Term Properties of Hot-Water Polyolefin Pipes – A Review", Polymer Engineering and Science, Vol. 34, No. 24, pp. 1773-1787.

Hsuan, Y.G. and Koerner, R.M. (1999), "Antioxidant Depletion Lifetime in High Density Polyethylene Geomembranes", Journal of Geotechnical and Geo-environmental Engineering, ASCE, Vol. 124, No. 6, pp. 532-541.

Hsuan, Y.G. and Guan, Z. (1998) "Antioxidant Depletion During thermal Oxidation of High Density Polyethylene Geomembranes", 6th International Conference on Geosynthetics, Atlanta, Georgia, USA, March, pp. 375-380.

Hsuan, Y.G. and McGrath, T.J. (1999). "HDPE Pipe: Recommended Material Specifications and Design Requirements," *NCHRP Report 429*, Transportation Research Board, National Research Council, Washington, DC.

Janson, L-E., (1995), *Plastics Pipes for Water Supply and Sewage Disposal*, Published by Borealis, 290 pgs.

Karlsson, K., Smith, G.D., and Gedde, U.W. (1992), "Molecular Structure, Morphology, and Antioxidant Consumption in Medium Density Polyethylene Pipes in Hot-Water Applications", *Polymer Engineering and Science*, Vol. 32, No. 10, pp. 649-657.

Popelar, C.F., Popelar, C.H. and Kenner, V.H. (1990), "Viscoelastic Material Characterization and Modeling for Polyethylene", *Polymer Engineering and Science*, Vol. 30, No. 10, pp. 577-586.

Popelar, C.H., Kenner, V.H. and Wooster, J.P. (1991), "An Accelerated Method for Establishing the Long Term Performance of Polyethylene Gas Pipe Materials", *Polymer Engineering and Science*, Vol. 31, No. 24, pp. 1693-1700.

Sangam, H.P. and Rowe, R.K. (2002), "Effects of Exposure Conditions on the Depletion of Antioxidants from High-Density Polyethylene (HDPE) Geomembranes", *Journal of Canadian Geotech.* 39, pp. 1221-1230.

Schmid, M. and Affolter, S. (2003), "Interlaboratory Tests on Polymers by Differential Scanning Calorimetry (DSC): Determination and Comparison of Oxidation Induction Time and Oxidation Induction Temperature", *Polymer Testing*, 22, pp. 419-428.

Smith, G.D., Karlsson, K., and Gedde, U.W., (1992), "Modeling of Antioxidant Loss From Polyolefins in Hot-Water Applications, I: Model and Application to Medium Density Polyethylene Pipes", *Polymer Engineering and Science*, Vol. 32, No. 1, pp. 658-667.

Viebke, J., Elble, E., Ifwarson, M., and Gedde, U.W. (1994), "Degradation of Unstabilized Medium-Density Polyethylene Pipes in Hot-Water Applications", *Polymer Engineering and Science*, Vol. 34, No. 17, pp. 1354-1361.

Viebke, J. and Gedde, U.W. (1994), "Assessment of Lifetime of Hot-Water Polyethylene Pipes Based on Oxidation Induction Time Data", *Polymer Engineering and Science*, Vol. 38, No. 8, pp. 1244-1250.